ARMY RESEARCH LABORATORY

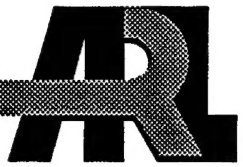

Induction Heating of Carbon-Fiber Composites: Thermal Generation Model

by Bruce K. Fink, Roy L. McCullough, and John W. Gillespie, Jr.

ARL-TR-2261 September 2000

The findings in this report are not to be construed as an official Department of the Army position unless so designated by other authorized documents.

Citation of manufacturer's or trade names does not constitute an official endorsement or approval of the use thereof.

Destroy this report when it is no longer needed. Do not return it to the originator.

Abstract

A theory of local and global mechanisms of heat generation and distribution in carbon-fiber-based composites subjected to an alternating magnetic field has been proposed. A model that predicts the strength and distribution of thermal generation through the thickness of carbon-fiber-based laminated composites has been developed. Earlier work has established the distribution of point voltages in the plane of the laminate that exist in the form of potential differences between fibers in adjacent plies in a cross-ply or angle-ply laminate system. In this work, a capacitive-layer microstructure that models the actual fiber-reinforced-polymer microstructure from a square-packing assumption to a series of conductive parallel plates is formulated. An effective parameter of heating, gamma, that establishes the distribution of heating through the thickness is defined. Extreme gradients in this thermal source can exist with peaks occurring at the interfaces of ply-ply orientation changes. An optimization study establishes the effect of various microstructural and macrostructural parameters on the heating parameter, gamma. Several parametric studies are performed on the computer algorithm, which calculates gamma to further analyze these effects.

Table of Contents

INTENTIONALLY LEFT BLANK.

List of Figures

INTENTIONALLY LEFT BLANK.

List of Tables

INTENTIONALLY LEFT BLANK.

1. Introduction

Induction heating involves the application of an alternating magnetic field that subjects an object to a distribution of magnetic flux. Experimental observations have shown that unidirectional carbon-fiber laminates subject to a uniform field do not heat. In contrast, cross-ply laminates exhibit significant heating. Two mechanisms of heating have been identified that result from an alternating rotational emf induced by the magnetic field: (1) joule losses in the carbon fibers induced by the eddy currents and (2) dielectric losses in the polymer. For joule losses to dominate heating, carbon fibers must be in good electrical contact with each other in adjacent layers of the cross-ply layer. Experiments have been conducted on cross-ply laminates that incorporate additional polymer interlayers. In this case, significant heating occurs for microstructures that eliminate fiber-fiber contact. This observation can be explained by proposing that the dominate mechanisms for localized heating result from dielectric losses in the matrix region separating fiber-fiber junctions, as illustrated in Figure 1 [1]. In this situation, a magnetic field B induces electric fields within the carbon fibers, creating a potential difference V across the polymeric region of thickness h. A "planar grid" model was developed to explore the consequence of local heating resulting from dielectric losses in the matrix [2]. In this model, two crossing layers of filaments separated by a polymer layer of thickness h were treated as a planar grid of capacitors. The transfer of energy from an applied magnetic field generated by a Helmholz coil was related to the resulting distribution of potential differences in the polymer plane separating the two layers. A nondimensional effective parameter of heating was introduced as the voltage per unit magnetic flux per unit frequency of the applied magnetic field.

Qualitative temperature distributions over the plane were observed by placing liquid crystals on the surface of a thin-section cross-plied carbon/polyetheretherketone laminate [2]. These observations showed local heating at the fiber crossover points, as predicted by the planar-grid capacitance model. Furthermore, the temperature distribution induced by a circular coil was in qualitative agreement with the predictions. Laminates were fabricated with various thicknesses of polymer layers between the laminae. The local heating at the fiber-fiber junctions persisted,

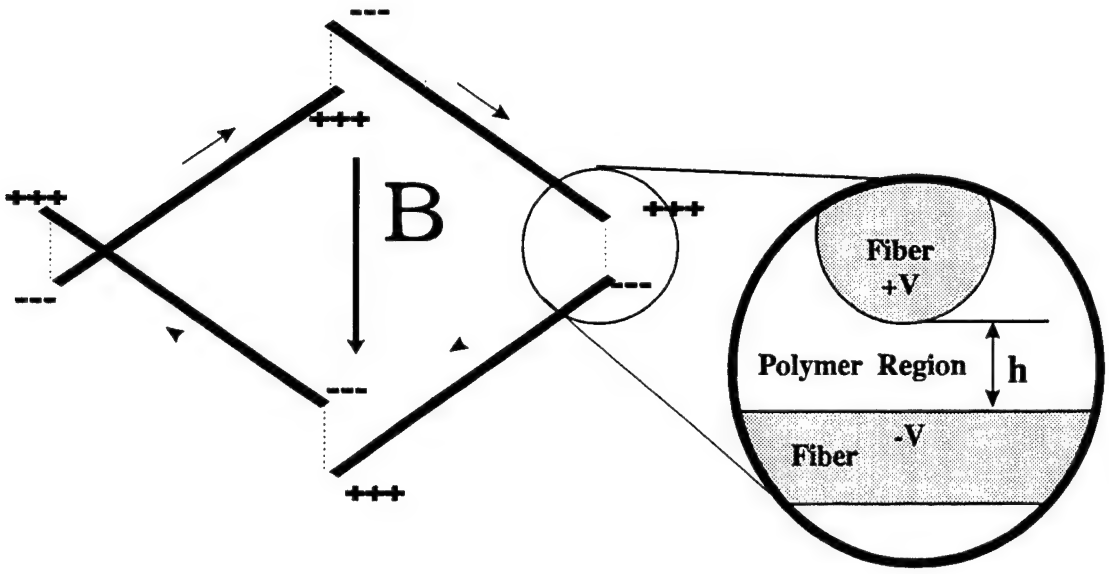

Figure 1. Induced Current Due to a Transverse (Normal to the Plane of Fibers) Magnetic Field B in a [0/90]s Cross-Ply. A Matrix-Rich Region of Thickness h Exists Between the Orthogonal Plies in Such a Laminate. A Potential Difference V Exists Between the Intersecting Fibers.

even though no fiber-fiber contacts were possible; however, as the thickness of the polymer layer was increased, the intensity of heating was diminished.

In this work, the previous treatment is extended to account for multilayer interactions that occur through the thickness in a carbon-based composite. Previous work modeled the interaction between single transverse fibers using an electric field concept [1] and the planar distribution of current based on an equivalent-resistance assumption [2] resulting in a qualitative view of thermal generation. In the present treatment, it is shown that the multilayer systems can give rise to complicated potential differences between the fibers through the thickness of the laminate. First, a capacitive layer analogy is developed and simplifications are introduced to provide estimates of the effective fields within the polymeric region that can be consolidated into an effective thickness parameter for the polymeric material. Through this approach, the effects of a complex distribution of potential differences can be captured in the form of a nondimensional heating parameter. Parametric studies based on this model identify the role of various microstructural features in the induction welding of carbon-fiber-based thermoplastic composites. Experimental evidence is presented to support these predictions.

2. Formulation

Figure 2 illustrates an idealized system of two orthogonal plies, each containing three fiber "layers," separated by a distance $h_0 = 2h_1$, as shown. In accordance with the planar grid model [2], each fiber layer pair between the adjacent plies of the 2-ply system is initially assumed to have the same potential difference. For example, the potential difference between fiber layer no. 3 in the 0° ply and fiber layer no. 3 in the 90° ply is initially assumed to be equivalent to the potential difference between fiber layer no. 3 in the 0° ply and fiber layer no. 2 in the 90° ply. Each of the $n^2 = 3^2 = 9$ fiber layer interactions is initially assumed to have the same potential difference as calculated by the planar-grid model. This implies that each fiber-fiber interaction creates a complicated electric field between two nonparallel conducting cylinders. As an example, for a 20-cm-square (~8 in.) 2-ply cross-ply laminated plate, there are approximately 2.5e + 11 interactions to consider. Consequently, a simplified model is needed to estimate the electric field in the polymeric regions and, in doing so, define an effective parameter for the thickness of polymeric material, h, through which the field acts.

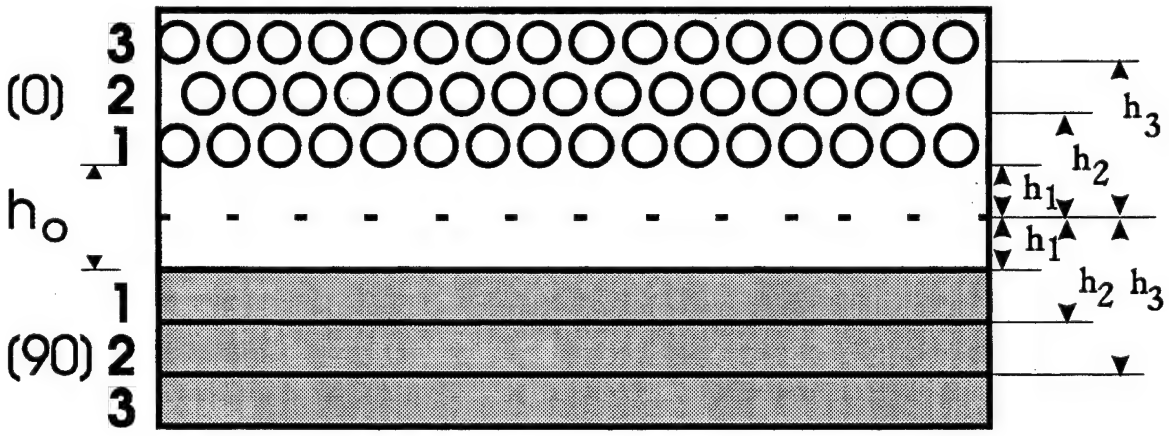

Figure 2. Simplified Representation of the Cross Section of a [0/90] Cross-Ply Laminate.

Electric field lines between fibers act almost entirely in the through-thickness sense, interacting with nearly all of the polymeric volume in the region between the two fibers. Under these conditions, it is plausible to represent rows of fibers as contiguous conductive material.

Furthermore, the fibers can be taken to be perfect conductors in comparison to the insulating polymer. With the assumption that the fiber volume fraction and laminate thickness are continuous in an elemental planar region, the electromagnetic interaction between two arbitrary fibrous layers can be treated as conductive plates separated by some particular distance, h.

Initially, consider just two such interacting conductive plates making up a "capacitive layer" pair in the x-y plane. A potential difference exists between the plates that is a function of the planar coordinates, x and y:

$$V(x,y) = -\int \vec{E}(x,y) \cdot d\vec{\ell} = E(x,y)h\,, \tag{1}$$

where E(x,y) is the electric field acting through the distance, h, separating the two plates. Therefore, a charge distribution exists:

$$q(x,y) = \varepsilon_o \kappa \oint \vec{E}(x,y) \cdot d\vec{S}\,, \tag{2}$$

where q(x,y) is the coulombic charge, ε_o is the permittivity of vacuum, κ is the relative dielectric constant of the material, and $\vec{S}$ is the Gaussian surface vector. If some elemental surface area ΔA is considered,

$$q(x,y)_A = \varepsilon_0 \kappa \Phi_E = \varepsilon_0 \kappa E(x,y) \Delta A \tag{3}$$

or

$$q(x,y)_{\Delta A} = \frac{\varepsilon_o \kappa \Delta A V(x,y)}{h}. \tag{4}$$

If ΔA is taken large enough such that its linear dimensions are much greater than h, the capacitance at the point (x,y) can be obtained:

$$C(x,y)_{\Delta A} = \frac{q(x,y)}{V(x,y)} = \frac{\varepsilon_o \kappa E(x,y)\Delta A}{E(x,y)h} = \frac{\varepsilon_o \kappa \Delta A}{h}. \quad (5)$$

The heating at point (x,y) can now be written as

$$W(x,y)_{\Delta A} = \omega \tan\delta \; C(x,y)_{\Delta A} V(x,y)^2, \quad (6)$$

where ω is the angular frequency of the electric field and $\tan\delta$ is the imaginary part of the complex dielectric constant for the polymer. Incorporating equation (5) for the capacitance yields

$$W(x,y)_{\Delta A} = \omega \tan\partial \frac{\varepsilon_0 \kappa \Delta A}{h} V(x,y)^2 = \frac{\beta V(x,y)^2}{h}. \quad (7)$$

Note that the quantity β/h is equivalent in units to 1/R, where R is a resistance indicating that dielectric heating follows a joule-type loss relationship. In the planar grid model of Fink, McCullough, and Gillespie [2], fairly large (2.5-cm square) element sizes (ΔA) were determined to be satisfactory representatives of the potential distribution for centered-coil problems. It was shown that the gradient in V(x,y) in the plane is much steeper for corner- or edge-placed coil arrangements due to the nature of eddy current formation in cross-ply laminates. Corner- or edge-placed coil arrangements require a finer mesh for accurate in-plane voltage analyses.

As noted previously, a through-thickness model must account for many parallel-plate capacitive interactions. Figure 3(a) illustrates three planar fiber layers above the 0°/90° interface and three below. The matrix interface region between the 0 and 90 is assigned a thickness of h_0; the thickness of the matrix layer within both the 0 and 90 regions is assigned the thickness d*. The quantity d* is dependent upon the volume fraction of fibers in a ply and the packing geometry. For this example, nine pair-wise fiber layer interaction combinations are possible. Each isolated pair initially carries the same potential difference, V(x,y); however, the separation distance, h, varies with each. For each isolated pair, the equation for heating, equation (6), holds. However, as the isolated pairs are brought

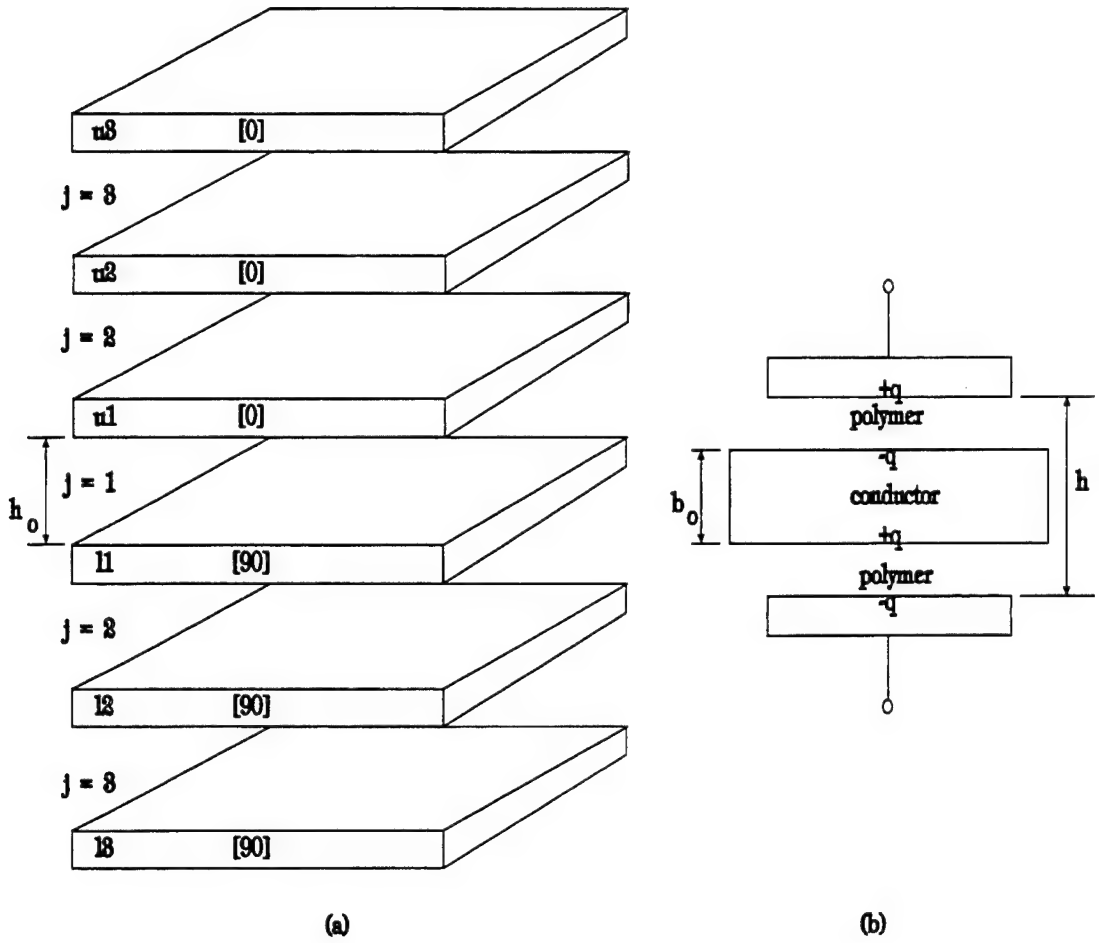

Figure 3. Series of Capacitive Layers Representing (a) a [0/90] Cross-Ply Laminate in Which Each Ply Consists of Only Three Fibers Through the Thickness on Average and (b) a Parallel Plate Capacitor With a Conductor Replacing Some of the Dielectric Material.

together to form the overall layered structure, the capacitance and voltage effectively change due to the presence of, N, intervening conducting fiber layers, each of thickness d_f^*, between the fiber layer pair under consideration.

The introduction of a conductive slab into a capacitor effectively decreases the distance between the charged plates. Figure 3(b) illustrates the situation in which a conductor is introduced within a capacitor containing a dielectric. A is the area of the charged plates in the capacitor, and q is the charge on each plate. Before the conductive slab is introduced,

$$C = \frac{\varepsilon_0 A \kappa}{h}, \tag{8}$$

and

$$V = \frac{q}{C} = \frac{qh}{\varepsilon_0 A \kappa}. \tag{9}$$

After the slab is introduced,

$$C_{new} = \frac{\varepsilon_0 A \kappa}{h - b_0} = \frac{C_{old}}{\left(1 - \frac{b_0}{h}\right)}, \tag{10}$$

and

$$V_{new} = \frac{q}{C_{new}} = V_{old}\left(1 - \frac{b_0}{h}\right), \tag{11}$$

where b_0 is defined in Figure 3(b) as the thickness of a conductive slab that replaces dielectric material in a parallel-plate capacitor. The capacitance is increased by the same amount that the potential difference is decreased. However, since heating is proportional to CV^2, the heating rate, from equation (6), is decreased by a factor of $(1 - b_{0/h})$. This decrease in heating can be accounted for by an effective (1/h) value for each possible fiber-fiber interaction through the thickness. In the following discussion, the quantity b_0 of Figure 3(b) is equivalent to the summation of effective thicknesses of fiber layers (conductive slabs) separating the two fiber layers under consideration.

The effect of several interactions can be illustrated for the [0/90] laminate of Figure 3(a). The plies of this laminate are assumed to have only three fiber layers for this discussion. The "upper" fiber layers are labeled u_1, u_2, and u_3 and the "lower" fiber layers are labeled l_1, l_2, and l_3. The thickness of

the region between the 0° and 90° plies is labeled h_0. The polymeric regions are labeled j = 1, 2, or 3. Table 1 summarizes the nine possible fiber-fiber interactions and the values of 1/h for each polymeric region between fiber planes. The quantity d* is the capacitive layer model's value for the distance between conductive plates (i.e., the thickness of the polymer regions).

Table 1. Individual Inverse Fiber-Fiber Interaction Distances for an Ideal Cross-Ply Laminate in Which Each Ply Consists of Three Fiber Layers Through the Thickness

	(1,1)	(1,2)	(1,3)	(2,1)	(2,2)	(2,3)	(3,1)	(3,2)	(3,3)	Total Per Polymeric Region
u_2 to u_3 j = 3							d*/B	d*/C	d*/D	$\sum_{a=2}^{2}\sum_{i=a}^{2+a}\frac{d^*}{(h_0+id^*)^2}$
u_1 to u_2 j = 2				d*/A	d*/B	d*/C	d*/B	d*/C	d*/D	$\sum_{a=1}^{2}\sum_{i=a}^{2+a}\frac{d^*}{(h_0+id^*)^2}$
u_1 to l_1 j = 1	$1/h_0$	h_0/A	h_0/B	h_0/A	h_0/B	h_0/C	h_0/B	h_0/C	h_0/D	$\sum_{a=0}^{2}\sum_{i=a}^{2+a}\frac{h_0}{(h_0+id^*)^2}$
l_1 to l_2 j = 2		d*/A	d*/B		d*/B	d*/C		d*/C	d*/D	$\sum_{a=1}^{2}\sum_{i=a}^{2+a}\frac{d^*}{(h_0+id^*)^2}$
l_2 to l_3 j = 3			d*/B			d*/C			d*/D	$\sum_{a=2}^{2}\sum_{i=a}^{2+a}\frac{d^*}{(h_0+id^*)^2}$
Total:										$\sum_{a=0}^{2}\sum_{i=a}^{2+a}\frac{1}{(h_0+id^*)}$

Notes: $A = (h_0 + d^*)^2$,
$B = (h_0 + 2d^*)^2$,
$C = (h_0 + 3d^*)^2$, and
$D = (h_0 + 4d^*)^2$.

The distance between u_1 and l_1 is h_0 and, since there are no other fibrous conductive layers between them, $1/h = 1/h_0$. For the interaction between u_1 and l_2, labeled as (1,2) in the table, there are two polymeric regions to consider but only one fiber-fiber interaction. The total distance between u_1 and l_2 is $h_0 + d^*$ so the total 1/h for this interaction is $1/(h_0 + d^*)$. However, the heat generation is divided between two polymeric regions; one region has thickness h_0 and the other has thickness d*.

Therefore, the fraction of heating in each is represented as $h_0/(h_0 + d^*)$ and $d^*/(h_0 + d^*)$, respectively. The total heating in each region, then, is given by

$$\left(\frac{1}{h}\right)_{j=1}^{(1,2)} = \frac{h_0}{h_0 + d^*}\frac{1}{h_0 + d^*} = \frac{h_0}{\left(h_0 + d^*\right)^2}, \tag{12}$$

and

$$\left(\frac{1}{h}\right)_{j=2}^{(1,2)} = \frac{d^*}{h_0 + d^*}\frac{1}{h_0 + d^*} = \frac{d^*}{\left(h_0 + d^*\right)^2} \tag{13}$$

for the j = 1 and j = 2 regions, respectively, of the (1,2) interaction. The remainder of Table 1 is completed accordingly. The column labeled "Total Per Polymeric Region" gives the total effective inverse distance for each polymer region taking into account all fiber-fiber interactions. The summation of these terms gives the total effective inverse h for the ply-ply interaction. From here on, this summation is termed the "gamma parameter" and is given the symbol γ_j for the j^{th} polymeric region through the thickness.

This example gives the results for a laminate with only three fiber layers above and below the ply-ply interface. The general case for a two-ply laminate consisting of m fiber layers in the "top" ply and n fiber layers in the "bottom" ply is given in equations (14) and (15) for the effective inverse h parameters γ_j and γ_{total}, respectively.

$$\left(\frac{1}{h}\right)_{j=1}^{eff} = \left(\frac{1}{h^*}\right)_1 = \sum_{a=0}^{m-1}\sum_{i=a}^{n+a-1}\frac{h_0}{\left(h_0 + id^*\right)^2}, \text{ and} \tag{14}$$

$$\left(\frac{1}{h}\right)_{j(m)}^{eff} = \left(\frac{1}{h^*}\right)_{j(m)} = \sum_{a=j-1}^{m-1}\sum_{i=a}^{n+a-1}\frac{d^*}{\left(h_0 + id^*\right)^2}, \tag{14a}$$

where j = 1, ..., m;

$$\left(\frac{1}{h}\right)_{j(n)}^{eff} = \left(\frac{1}{h^*}\right)_{j(n)} = \sum_{a=j-1}^{n-1} \sum_{i=a}^{m+a-1} \frac{d^*}{(h_0 + id^*)^2}, \tag{14b}$$

where j = 1, ..., n; and

$$\left(\frac{1}{h}\right)_{total}^{eff} = \left(\frac{1}{h^*}\right)_{total} = \sum_{a=0}^{m-1n+a-1} \sum_{i=a} \frac{1}{(h_0 + id^*)}. \tag{15}$$

Equations (14a) and (14b) are identical if m = n.

Quantities of special interest are the thermal energy (heating) at the interface of two adjacent plies represented by γ_1, the total heating in the two-ply laminate represented by γ_{total}, and the ratio of these values, which represents the fraction of total heating that occurs in the interface region. To qualitatively evaluate the role of these parameters, it is useful to replace equations (14) and (15) by integral forms; viz.,

$$\gamma_1 \cong \frac{1}{d^*} \int_{a=0}^{(m-1)(n+a-1)} \int_{i=a} \frac{b}{(b+i)^2} dida, \tag{16}$$

where $b = h_0/d^*$. Equation (16) can be approximated as

$$\gamma_1 \cong \frac{1}{d^*} b \ln\left[\frac{(b+m-1)(b+n-1)}{b(b+n+m-2)}\right]. \tag{17}$$

For the case where m = n, this can be further reduced to

$$\gamma_1 \cong \frac{1}{d^*} b \ln\left[\frac{(b+n-1)^2}{b(b+2n-2)}\right]. \tag{18}$$

Likewise, for the total effective inverse h,

$$\gamma_{total} \cong \frac{1}{d^*}[(r\ln r - r) - (s\ln s - s) - (t\ln t - t) + (b\ln b - b)], \tag{19}$$

where

$r = b + n + m - 2,$

$s = b + m - 1,$ and

$t = b + n - 1.$

For the case where $m = n$,

$$\gamma_{total} \cong \frac{1}{d^*}(g\ln g - 2h\ln h + b\ln b), \tag{20}$$

$g = b + 2n - 2,$ and

$h = b + n - 1.$

The optimization of overall energy production is obtained by the maximization of equations (17) and (19). These conditions yield the requirement that $m = n$ be maximized and h_0 be minimized.

If equations (18) and (20) are divided by the volumes over which they act and the ratio of the two taken, the ratio of heating is obtained at the interface to heating in the laminate (equation [21]). In welding operations, it may be desirable to preferentially (or nonpreferentially) heat the interface so this ratio should be as large (or small) as possible.

$$\frac{\gamma_1}{\gamma_{total}} = \frac{\frac{\gamma_1}{b}}{2Z - \frac{\gamma_1}{b + 2n}}, \tag{21}$$

where

$$Z = \frac{1}{b+2n}(n-1)\ln\left(\frac{b+2n-2}{b+n-1}\right).$$

Maximization requires that ply thicknesses, m = n, be maximized and that the interface thickness, h_0, be minimized as before. Therefore, increasing heating by either increasing ply thickness or decreasing h_0 also increases the preferential nature of heating at the interface.

As implied earlier, the quantity d* is related to the volume fraction fiber (X_f) and the fiber-packing geometry. Several ideal packing geometries exist; the most common are rectangular, square, and hexagonal. A square-packing assumption was used for this study for simplicity and adaptability to the capacitive-layer model. As a caveat for this assumption, rectangular and hexagonal packing geometries were analyzed separately and, with deference to the more straightforward square-packing geometry, were found to have no significant influence on the through-thickness potential difference results when realistic thicknesses of composite laminates were considered. Figure 4(a) shows the parameters involved and Figure 4(b) shows the modeled system with its corresponding parameters. The quantity a is the dimension of the unit cell and is equivalent to the summation of the fiber diameter d_f and the distance between fibers d. The quantities d_f* and d* are the fiber diameter and fiber separation dimensions corresponding to the model's unit cell. The unit cell dimension a is taken to be constant, establishing the condition that

$$d + d_f = d^* + d_f^* \tag{22}$$

and the fiber volume fraction remains constant, requiring that,

$$X_f = \frac{d_f^*}{d^* + d_f^*}. \tag{23}$$

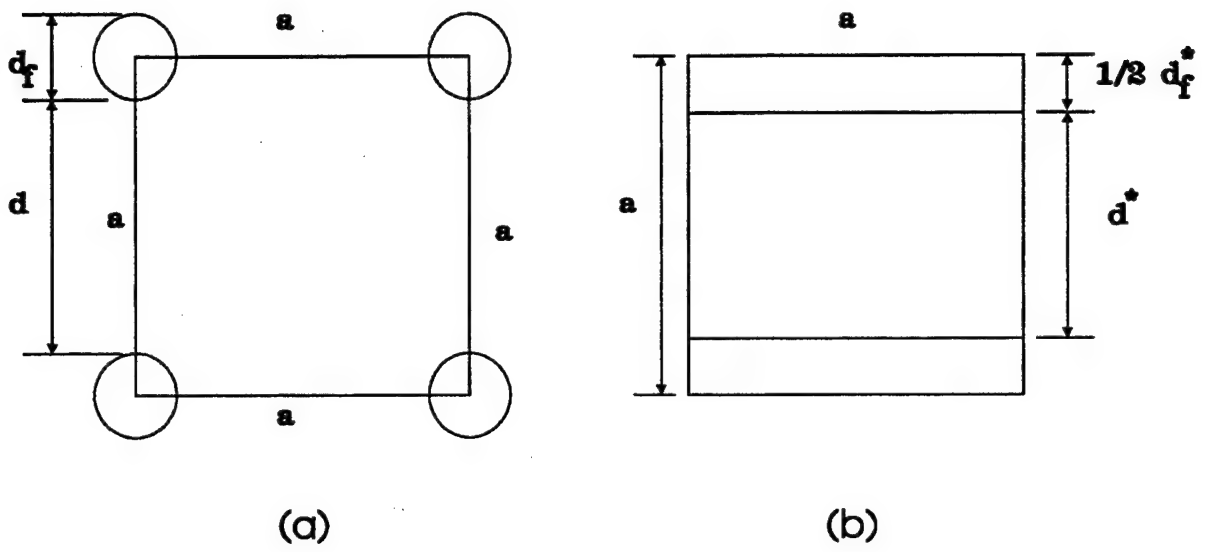

Figure 4. Unit Cells for (a) Square-Packing Assumption and (b) Capacitive-Plate Assumption.

Equation (23) can be used to specify d* in terms of the fiber volume fraction X_f. Combining Equations (22) and (23) gives d* in terms of the microstructural parameters d and d_f,

$$d^* = (1 - X_f)(d + d_f). \tag{24}$$

For the square-packing geometry,

$$X_f = \frac{\pi d_f^2}{4(d + d_f)^2}. \tag{25}$$

Combining these relationships yields the effective interlayer distance d* in terms of the microstructural parameters:

$$d^* = \frac{(1 - X_f)\sqrt{\pi} d_f}{2\sqrt{X_f}}. \tag{26}$$

The question arises as to how many fiber layers are necessary for the square-packed/capacitive-layer model to be appropriate. The condition of uniform fiber volume fraction (equation [23]) is not necessarily met when the number of fiber layers, n, is low. Equation (27) gives the ratio of effective polymer thickness to total thickness for the square-packed model:

$$\frac{t_{eff}}{t} = \frac{(n-1)d^*}{(n-1)d^* + nd_f^*}. \tag{27}$$

Figure 5 shows the plot of equation (27) (with $X_f = 0.60$) vs. n, indicating a convergence to the expected value of 0.40. APC-2 has a fiber volume fraction of approximately 0.60 and each prepreg ply has between 16 and 20 fiber layers upon consolidation. The results of Figure 5 indicate that it is plausible to use the capacitive-layer model for laminates of nominally one ply and greater.

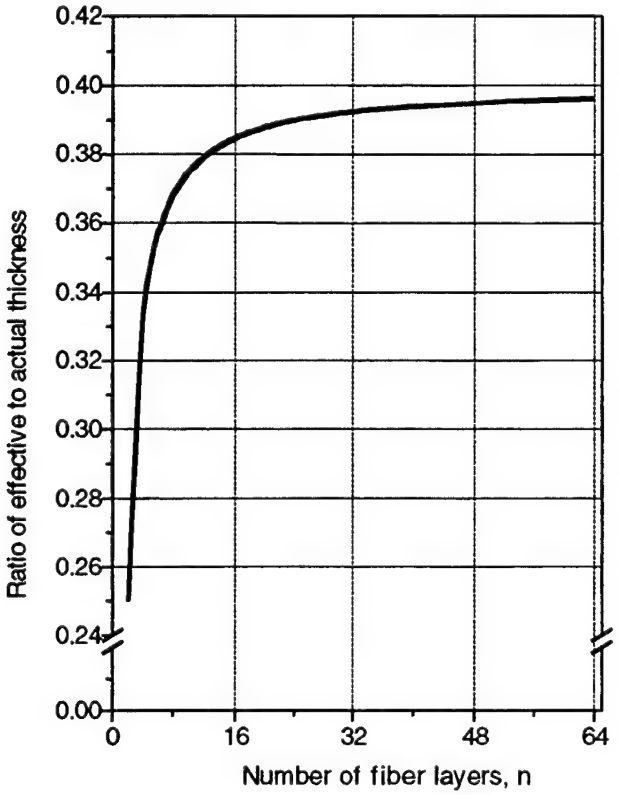

Figure 5. Plot of Equation (27) Showing the Convergence of the Ratio of Effective to Actual Thickness in the Square-Packed Capacitive-Layer Model for Fiber-Fiber Interactions Through the Thickness of a Laminate Consisting of n Fiber Layers.

3. Model Predictions

Figure 6 shows an outline of a computer algorithm used to determine the effective heating parameter γ. Blocks 1 and 2 are based on the relationships previously discussed. Block 3 is the summation of the ply-ply interactions. Most case studies were performed using laminates with only one change in ply orientation through the thickness. The program calculates $\gamma_j d^*$, where j is defined in Figure 3. The quantity $b = h_0/d^*$ is used so that all calculated quantities are in terms of the model's capacitive-layer separation distance d*, and the result is nondimensional.

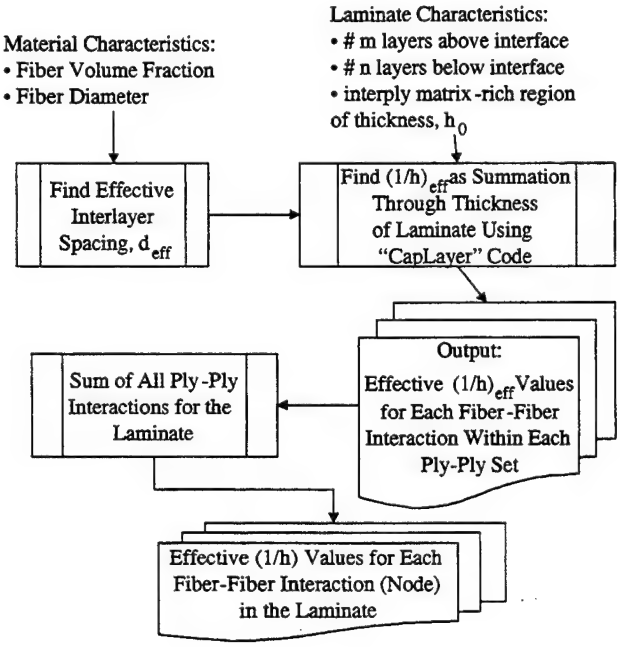

Figure 6. Outline of Capacitive-Layer Computer Algorithm.

3.1 Effect of Interply Thickness. Three relevant cases for polymer thickness of h_0 = 125 μm, 25 μm, and 3.2 μm are presented as examples of model prediction. Table 2 provides the program input parameters for the three cases. The calculations described to this point do not take into account the distribution of heating per unit thickness of the regions j. Since region j = 1 is of thickness h_0 and regions j = 2, . . ., n or m are of thickness d*, the normalized γd^* values are used. The ratio of

interfacial heating to total heating in the ply-ply interface region is given in Table 3 for each case. As the interply matrix-rich region decreases, γ_{total} increases, as expected, and γ_i decreases. Heating, however, is a function of the volume of material to which energy is being supplied; so, as the third and fourth columns of Table 3 indicate, the normalized output representing heating increases for the entire laminate (at even faster rates) with decreasing interply thickness, h_0. The fifth column indicates the ratio of interface to total laminate heating, as defined in equation (21). The high ratio drops off rapidly with increasing interply thickness. Consequently, maximum interfacial heating is expected to occur when the thickness of the laminate is maximized and the thickness of the interfacial polymer is minimized.

Table 2. Input Parameters for Case Studies of Fiber-Fiber Submodel. $X_f = 0.60$, $d_f = 7$ μm, 20 Fiber Layers Per Ply, and $d^* = 3.2$ μm.

Case	0° Ply Layers, m	90° Ply Layers, n	Interply Thickness, h_0	$b = h_0/d^*$
1	60	60	125 μm (5 mil)	40
2	60	60	25 μm (1 mil)	8
3	60	60	3.2 μm (1/8 mil)	1

Table 3. Comparison of γ_{total} and γ_i for the Example Cases in the Fiber-Fiber Submodel. Normalization Occurs Against the Ratio of Interface Thickness to Effective Fiber Layer Spacing From Table 2.

Case	$b = h_0/d^*$	(1) $\gamma_i d^*$	(2) $\gamma_{total} d^*$	(3) Normalized $\gamma_i d^*$	(4) Normalized $\gamma_{total} d^*$	(5) γ_i/γ_{total} Ratio of Col. (3) to (4)
1	40	18.31	28.66	0.46	0.18	2.55
2	8	12.95	65.39	1.62	0.57	3.18
3	1	4.98	82.68	4.98	0.68	7.32

A parametric study was performed to ascertain the effect of varying the interply thickness, h_0, while maintaining a constant ply thickness of a single ply on either side of the ply-ply interface ([0/90]). Values of $d_f = 7$ μm, $X_f = 0.60$, and $m = n = 20$ were input into the model with various

values of $b = h_0/d^*$. The values for fiber diameter and fiber volume fraction are within the range of values reported by the manufacturer and in the literature [3–5] and the number of fibers through the thickness is within the range of values determined in a micrographical study [6]. Graphical results are presented in Figures 7 and 8. Figure 7 plots nondimensionalized "energy" input to the total laminate and the "center" interply region vs. nondimensionalized interply thickness. The series solution is the exact solution of the model. The integral solution is provided to qualify its use in the optimization study.

Note that, at low interply thickness ($b<\sim13$) in Figure 7, the energy production in the interply region increases with increasing h_0 then decreases slowly past that point.

From equation (21), the ratio of total energy input to the resin-rich interply region to total energy input to the entire laminate was examined and found to increase as the interply region increased. Figure 7 indicates this trend since the total energy input into the interply region is significantly lower than that of the laminate and the ratio decreases significantly with increasing interply thickness. This difference is shown quantitatively in Figure 8 as the ratio of specific energy or heating in the interply region to that in the laminate (per unit thickness). Figure 8 illustrates the important relationship of increasing localization of heating with decreasing interply resin thickness.

3.2 Varying Ply Thickness. Increasing the thickness of the 0° and 90° plies within the laminate has the opposite overall effect of independently increasing the interply thickness. The results of a parametric study involving several $[0_m/90_n]$ cases are graphically depicted in Figures 9 and 10, where the y-axis variables are equivalent to Figures 7 and 8, respectively, of the last section.

A comparison of Figure 10 with Figure 8 shows that it is beneficial to decrease the thickness of the polymer interply region while increasing the number of plies for maximized interfacial heating. A slight decrease in h_0 can possibly produce more significant increases in heating than can a larger magnitude increase in the ply thickness. Figure 8 suggests that heating can be controlled by careful

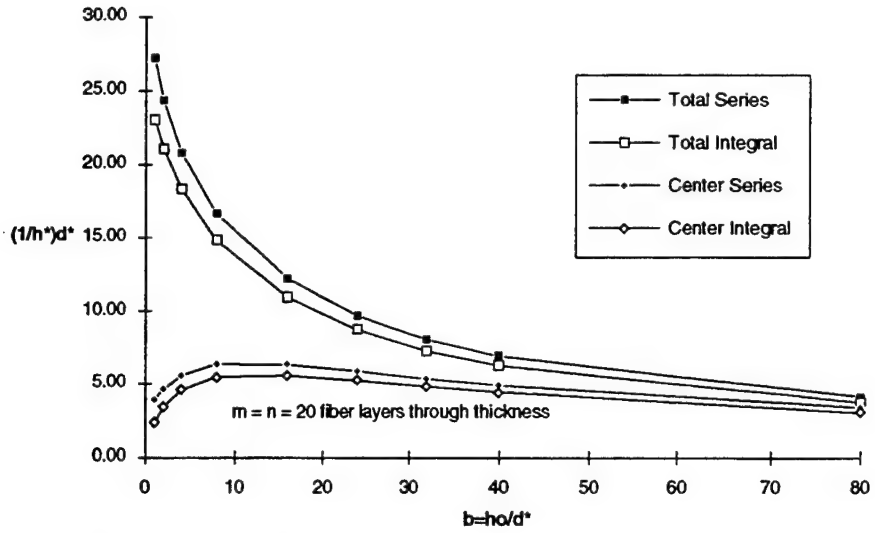

Figure 7. Results of Parametric Study of Capacitive-Layer Model to Determine Effects of Increasing Interply Resin Thickness on Dimensionless Heating Parameter. Comparison of Interface Energy Input (γ/d^*) to Total Energy Input ($\gamma_{total}d^*$) for Both the Exact Series Solution and the Approximate Integral Solution.

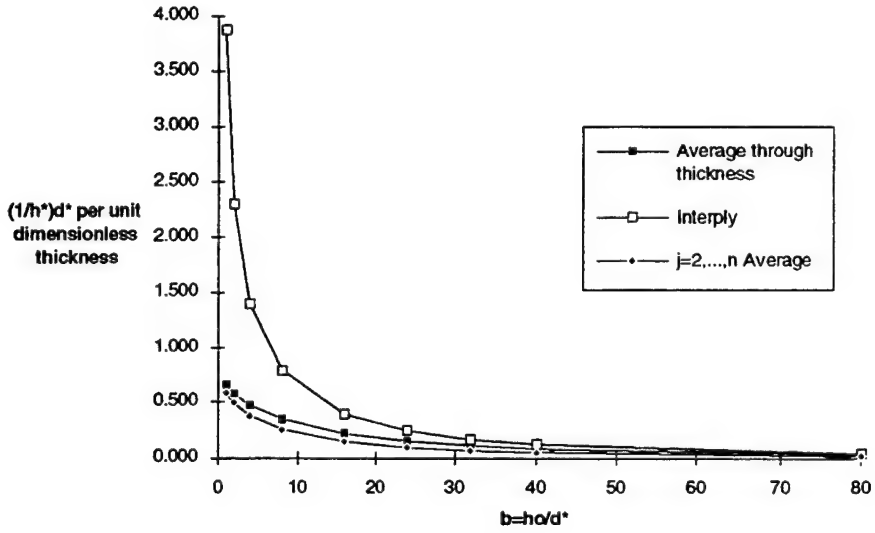

Figure 8. Results of Parametric Study of Capacitive-Layer Model to Determine Effects of Increasing Interface Resin Thickness h_0 on Dimensionless Heating Parameter γ. Ratio of Center to Average Interfiber Heating, $\gamma_1/[(\gamma_{total}-\gamma_1)/_{(m+n)}]$, Plotted Against Increasing Interface Thickness. This Represents the Multiplicity of Average Interfiber Heating That Is Consumed by the Interply Resin. For Example, at b = 1, Which Represents an Interply Thickness Equal to d*, the Heating in the Interply Resin Rich Region Is Approximately Six Times the Average Heating in the Rest of the Laminate.

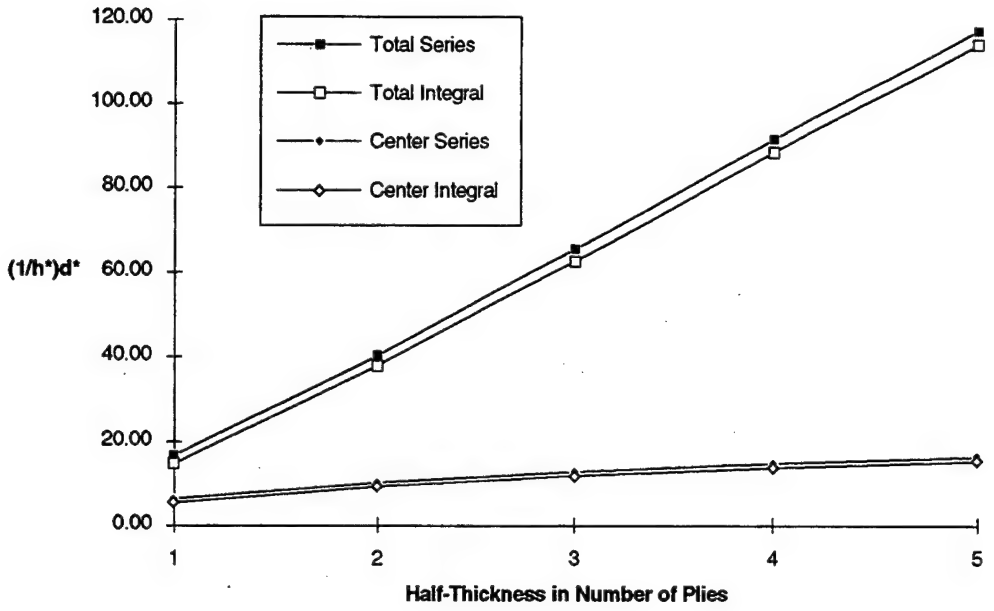

Figure 9. Comparison of Interface "Energy Input" ($\gamma_1 d^*$) to Total "Energy Input" ($\gamma_{total} d^*$) for Both Exact Series Solution and Approximate Integral Solution.

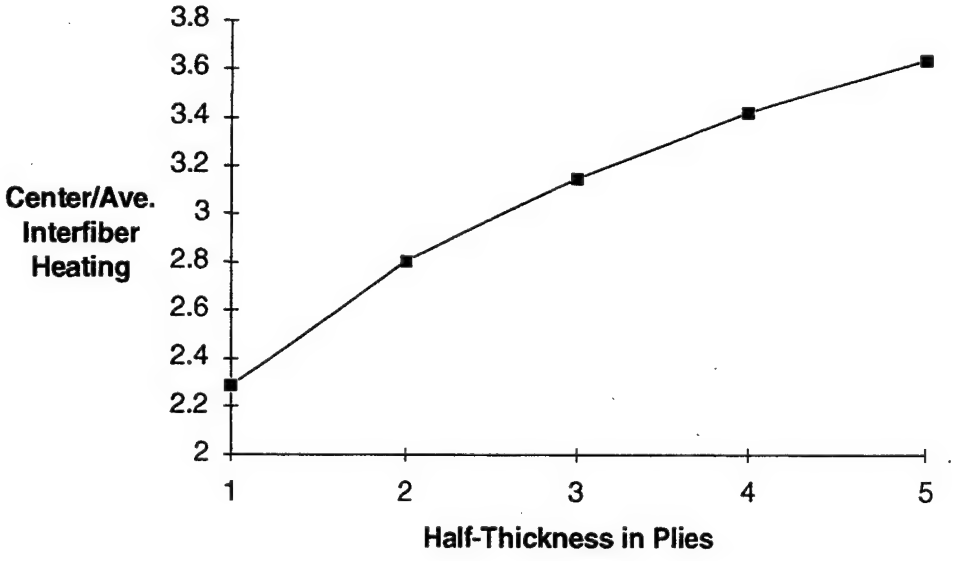

Figure 10. Ratio of Center to Average Interfiber "Heating," $\gamma_1/[(\gamma_{total}-\gamma_1)/_{(m+n)}]$, Plotted Against Increasing Ply Thickness. This Represents the Multiplicity of Average Interfiber Heating That Is Consumed by the Interply Resin. For Example, at a Laminate Thickness of 2 Plies (Half-Thickness = 1), the Heating in the Interply Resin-Rich Region Is Approximately 2.3 Times the Average Heating in the Rest of the Laminate.

control of the thickness of the resin-rich interply region—a relatively easy parameter to control in processing, although with possible detrimental effects on mechanical properties for large h_0.

4. Discussion

While the model presented in this paper determines the through-thickness distribution of the effective parameter of heating γ, it must be combined with the planar voltage distribution model [2], the local heat-generation model [1], and a finite element heat-transfer model [6], which, together, yield the thermal distribution of heating at the surface of the laminate. Extensive testing that strongly supports the combined models' predictions has been performed. The details of the experimental procedure used and a comprehensive verification of the global model [6] have been provided separately. A full discussion of the testing procedure and the other models is not within the scope of this paper; however, a few results are provided to initially verify the through-thickness model as a component of the global model, as well as the validity of the dielectric loss mechanism.

The two key parameters discussed previously are the polymeric interface thickness and the actual ply thickness (or number of plies) in a ply-ply interaction. The predicted effect of varying the interface thickness on the heating parameter γ (Figure 8) indicated a rapid decrease in γ with increasing interface resin thickness h_0. Figure 11 compares predicted and experimental steady-state surface temperatures at one point for [0/90] specimens manufactured with varying thicknesses of interply polymer. The experimental error bars (heavy lines) are indicative of the ± 1 °C reading of the digital thermocouple and an additional $\pm 5\%$ error on the accuracy of the placement of the thermocouple. The theoretical results' error bars (light lines) are the results of the application of upper and lower bounds on all known parameters, including geometrical and material property characteristics. Similar results in consideration of the ply thickness are shown in Figure 12. While these results do not provide a direct proof of the proposed model, they do provide persuasive evidence supporting the combined models' foundation.

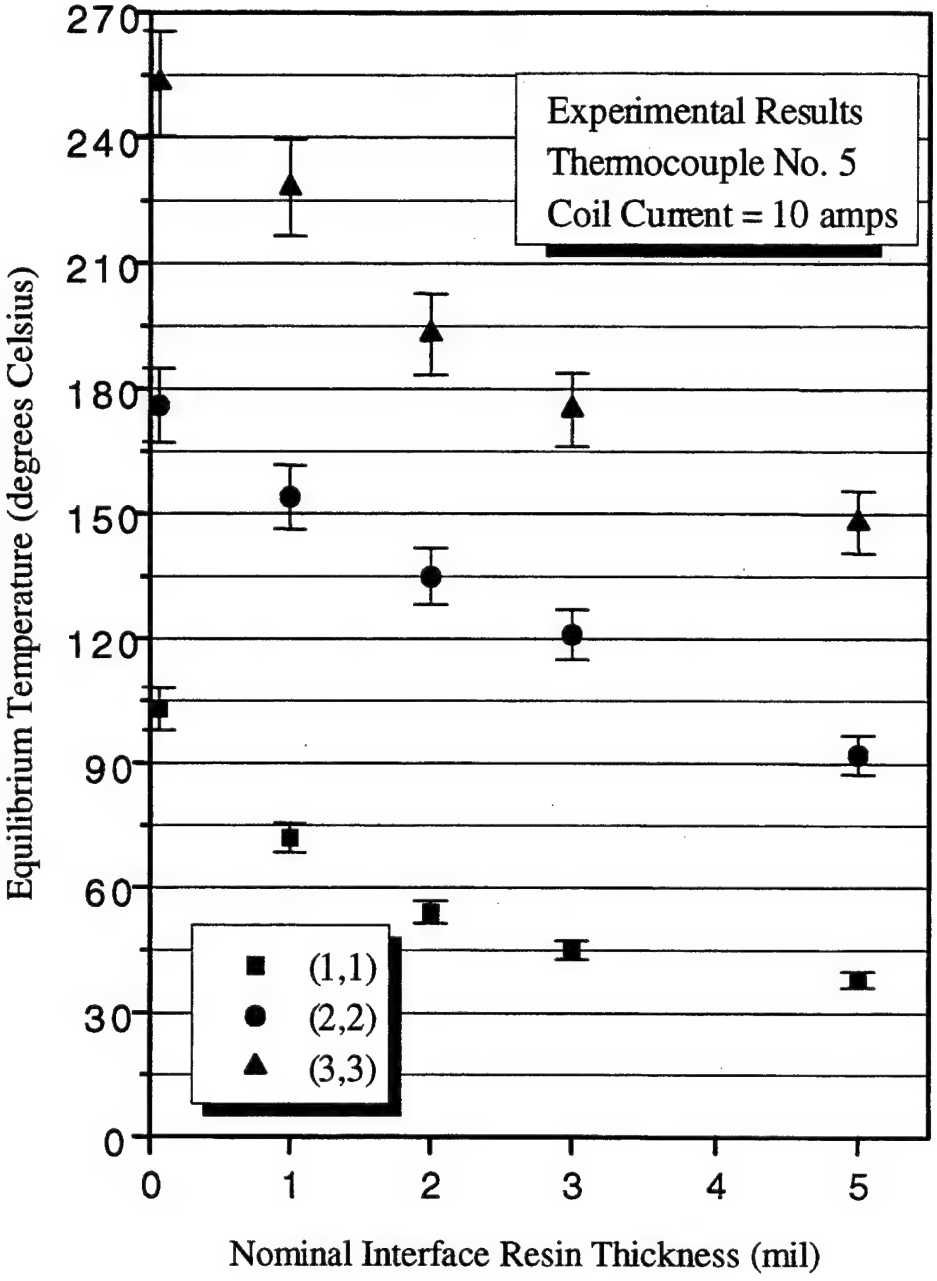

Figure 11. Comparison of Predicted and Observed Surface Temperatures Showing Effect of Increasing Interface Thickness (h_0) on Equilibrium Surface Temperature. The Heavy Lines Represent the Experimental Results While the Thin Lines Represent Predicted Results With Upper and Lower Bounds.

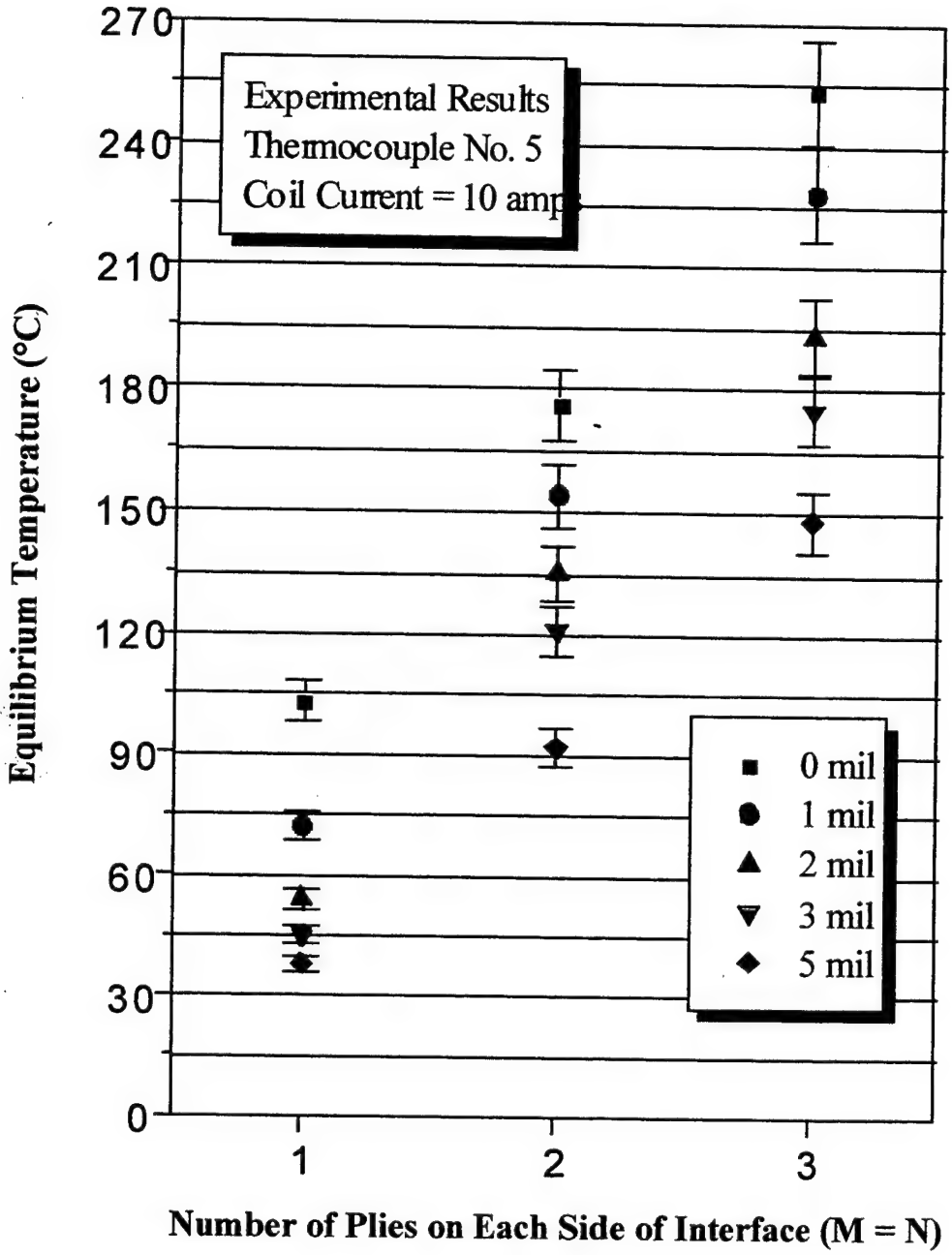

Figure 12. Comparison of Predicted and Observed Surface Temperatures Showing Effect of Increasing the Number of Plies on Each Side of the Interface. The Heavy Lines Represent the Experimental Results While the Thin Lines Represent Predicted Results With Upper and Lower Bounds.

Other observations further support the dominate role of dielectric losses rather than joule losses in the induction heating of carbon-fiber composites. As indicated previously, observed heating patterns show significant heating only where conductive paths overlap. Different polymers were used to separate carbon-fiber laminae. Heating characteristic changed with the change in polymer interlayer. This supports the proposal that heating is due to dielectric losses in the polymer since the dielectric behavior of the polymers (PEEK and PEI) have different dielectric loss spectra. An alternate explanation for the heating behavior could be attributed to dielectric breakdown in the thin polymer layers between fibers. Such a breakdown would provide conducting paths to connect the conducting carbon fibers. However, cycle tests show no change in heating rate between the first cycle and later cycles. If dielectric breakdown had occurred, the later cycles should have exhibited different heating characteristics. The fact that rapid heating is attainable at relatively large interply thicknesses further discounts the role of dielectric breakdown, as well as charge transfer mechanisms.

5. Summary

A capacitive-layer model has been developed to establish the mechanisms for fiber-layer interaction. The model uses a capacitive-layer parallel-plate assumption to develop the equations that describe the electromagnetic interaction between fibers in adjacent plies and the resulting reaction of the interply and interfiber polymeric regions to the induced electric fields. This model effectively incorporates the key microstructural (fiber diameter, fiber volume fraction) and macrostructural (interply thickness, laminate thickness) characteristics of the laminated plate. Each of these parameters affects the heating in a manner independently predicted by the capacitive-layer model. The model utilizes a nondimensional parameter, which represents the thermal generation within a ply-ply interaction. This parameter, γd^*, was then normalized with respect to volume for comparison with other systems and between polymeric regions within the laminate. Note that the model initially assumes that each opposing fiber-fiber pair is separate from its neighbors and carries an equivalent voltage, V_{xy}. When the model superimposes the system of fibers into its actual form, the actual voltage distribution is proportional to the square root of γ times the equivalent voltage V_{xy}.

Parametric studies identified the desired extremes of key parameters for overall thermal generation and preferential (or nonpreferential) heating in the ply-ply interface region. These studies showed that, in order to maximize the heating at any point in the plane of the cross-ply or angle-ply laminate, the fiber volume fraction should be maximized, the fiber diameter should be minimized, the interply resin thickness should be minimized, and the ply thickness above and below the interface should be maximized. This model has been indirectly verified through a global model analysis and the execution of a rigorous experimental matrix.

6. References

1. Fink, B. K., R. L. McCullough, and J. W. Gillespie, Jr. "A Local Theory of Heating in Cross-Ply Carbon Fiber Thermoplastic Composites by Magnetic Induction." *Polymer Engineering and Science*, vol. 32, no. 5, p. 357, 1992.

2. Fink, B. K., R. L. McCullough, and J. W. Gillespie, Jr. "A Model to Predict the Planar Electrical Potential Distribution in Cross-Ply Carbon-Fiber Composites Subjected to Alternating Magnetic Fields." *Computer Science Technology*, vol. 49, p. 71, 1993.

3. Jakobsen, T. B., R. D. Don, and J. W. Gillespie, Jr. "Two-Dimensional Thermal Analysis of Resistance Welded Thermoplastic Composites." *Polymer Engineering and Science*, vol. 29, no. 23, 1989.

4. Hercules, Inc. "Magnamite Graphite Fiber Type AS4." Provo, UT, 1990.

5. ICI Fiberite. "Property Data of Aromatic Polymer Composite: APC-2/Hercules Magnamite AS-4 Carbon Fiber." Leeds, United Kingdom, 1986.

6. Fink, B. K. "Heating of Continuous-Carbon-Fiber Thermoplatic-Matrix Composites by Magnetic Induction." Ph.D. dissertation, University of Delaware, Newark, DE, 1991.

INTENTIONALLY LEFT BLANK.

NO. OF COPIES	ORGANIZATION
2	DEFENSE TECHNICAL INFORMATION CENTER DTIC DDA 8725 JOHN J KINGMAN RD STE 0944 FT BELVOIR VA 22060-6218
1	HQDA DAMO FDT 400 ARMY PENTAGON WASHINGTON DC 20310-0460
1	OSD OUSD(A&T)/ODDDR&E(R) R J TREW THE PENTAGON WASHINGTON DC 20301-7100
1	DPTY CG FOR RDA US ARMY MATERIEL CMD AMCRDA 5001 EISENHOWER AVE ALEXANDRIA VA 22333-0001
1	INST FOR ADVNCD TCHNLGY THE UNIV OF TEXAS AT AUSTIN PO BOX 202797 AUSTIN TX 78720-2797
1	DARPA B KASPAR 3701 N FAIRFAX DR ARLINGTON VA 22203-1714
1	NAVAL SURFACE WARFARE CTR CODE B07 J PENNELLA 17320 DAHLGREN RD BLDG 1470 RM 1101 DAHLGREN VA 22448-5100
1	US MILITARY ACADEMY MATH SCI CTR OF EXCELLENCE DEPT OF MATHEMATICAL SCI MADN MATH THAYER HALL WEST POINT NY 10996-1786

NO. OF COPIES	ORGANIZATION
1	DIRECTOR US ARMY RESEARCH LAB AMSRL D D R SMITH 2800 POWDER MILL RD ADELPHI MD 20783-1197
1	DIRECTOR US ARMY RESEARCH LAB AMSRL DD 2800 POWDER MILL RD ADELPHI MD 20783-1197
1	DIRECTOR US ARMY RESEARCH LAB AMSRL CS AS (RECORDS MGMT) 2800 POWDER MILL RD ADELPHI MD 20783-1145
3	DIRECTOR US ARMY RESEARCH LAB AMSRL CI LL 2800 POWDER MILL RD ADELPHI MD 20783-1145
	ABERDEEN PROVING GROUND
4	DIR USARL AMSRL CI LP (BLDG 305)

NO. OF COPIES	ORGANIZATION
1	DIRECTOR US ARMY RESEARCH LAB AMSRL CP CA D SNIDER 2800 POWDER MILL RD ADELPHI MD 20783-1145
1	DIRECTOR US ARMY RESEARCH LAB AMSRL OP SD TA 2800 POWDER MILL ROAD ADELPHI MD 20783-1145
3	DIRECTOR US ARMY RESEARCH LAB AMSRL OP SD TL 2800 POWDER MILL ROAD ADELPHI MD 20783-1145
1	DIRECTOR US ARMY RESEARCH LAB AMSRL OP SD TP 2800 POWDER MILL ROAD ADELPHI MD 20783-1145
2	DIRECTOR US ARMY RESEARCH LAB AMSRL OP CI AD TECH PUB BR RECORDS MGMT ADMIN 2800 POWDER MILL ROAD ADELPHI MD 20783-1197
1	HQDA DAMI FIT NOLAN BLDG WASHINGTON DC 20310-1025
1	DIRECTOR DA OASARDA SARD SO 103 ARMY PENTAGON WASHINGTON DC 20310-0103
1	DEPUTY ASST SCY FOR R&T SARD TT RM 3EA79 THE PENTAGON WASHINGTON DC 20301-7100

NO. OF COPIES	ORGANIZATION
1	COMMANDER US ARMY MATERIEL CMD AMXMI INT 5001 EISENHOWER AVE ALEXANDRIA VA 22333-0001
2	COMMANDER US ARMY ARDEC AMSTA AR AE WW E BAKER J PEARSON PICATINNY ARSENAL NJ 07806-5000
1	COMMANDER US ARMY ARDEC AMSTA AR TD C SPINELLI PICATINNY ARSENAL NJ 07806-5000
1	COMMANDER US ARMY ARDEC AMSTA AR FSE T GORA PICATINNY ARSENAL NJ
6	COMMANDER US ARMY ARDEC AMSTA AR CCH A W ANDREWS S MUSALLI R CARR M LUCIANO E LOGSDEN T LOUZEIRO PICATINNY ARSENAL NJ 07806-5000
4	COMMANDER US ARMY ARDEC AMSTA AR CC G PAYNE J GEHBAUER C BAULIEU H OPAT PICATINNY ARSENAL NJ 07806-5000

NO. OF COPIES	ORGANIZATION
1	COMMANDER US ARMY ARDEC AMSTA AR CCH P J LUTZ PICATINNY ARSENAL NJ 07806-5000
1	COMMANDER US ARMY ARDEC AMSTA AR FSF T C LIVECCHIA PICATINNY ARSENAL NJ 07806-5000
1	COMMANDER US ARMY ARDEC AMSTA AR QAC T C C PATEL PICATINNY ARSENAL NJ 07806-5000
2	COMMANDER US ARMY ARDEC AMSTA AR M D DEMELLA F DIORIO PICATINNY ARSENAL NJ 07806-5000
3	COMMANDER US ARMY ARDEC AMSTA AR FSA A WARNASH B MACHAK M CHIEFA PICATINNY ARSENAL NJ 07806-5000
2	COMMANDER US ARMY ARDEC AMSTA AR FSP G M SCHIKSNIS D CARLUCCI PICATINNY ARSENAL NJ 07806-5000

NO. OF COPIES	ORGANIZATION
1	COMMANDER US ARMY ARDEC AMSTA AR FSP A P KISATSKY PICATINNY ARSENAL NJ 07806-5000
2	COMMANDER US ARMY ARDEC AMSTA AR CCH C H CHANIN S CHICO PICATINNY ARSENAL NJ 07806-5000
9	COMMANDER US ARMY ARDEC AMSTA AR CCH B P DONADIA F DONLON P VALENTI C KNUTSON G EUSTICE S PATEL G WAGNECZ R SAYER F CHANG PICATINNY ARSENAL NJ 07806-5000
6	COMMANDER US ARMY ARDEC AMSTA AR CCL F PUZYCKI R MCHUGH D CONWAY E JAROSZEWSKI R SCHLENNER M CLUNE PICATINNY ARSENAL NJ 07806-5000
1	COMMANDER US ARMY ARDEC AMSTA AR QAC T D RIGOGLIOSO PICATINNY ARSENAL NJ 07806-5000

NO. OF COPIES	ORGANIZATION
1	COMMANDER US ARMY ARDEC AMSTA AR SRE D YEE PICATINNY ARSENAL NJ 07806-5000
1	COMMANDER US ARMY ARDEC AMSTA AR WET T SACHAR BLDG 172 PICATINNY ARSENAL NJ 07806-5000
1	COMMANDER US ARMY ARDEC SMCAR ASF PICATINNY ARSENAL NJ 07806-5000
1	COMMANDER US ARMY ARDEC AMSTA AR WEL F INTELLIGENCE SPECIALIST M GUERRIERE PICATINNY ARSENAL NJ 07806-5000
11	PROJECT MANAGER US ARMY TMAS SFAE GSSC TMA R MORRIS C KIMKER D GUZOWICZ E KOPACZ R ROESER R DARCY R MCDANOLDS L D ULISSE C ROLLER J MCGREEN B PATTER PICATINNY ARSENAL NJ 07806-5000

NO. OF COPIES	ORGANIZATION
2	PEO FIELD ARTILLERY SYSTEMS SFAE FAS PM H GOLDMAN T MCWILLIAMS PICATINNY ARSENAL NJ 07806-5000
6	PM SADARM SFAE GCSS SD COL B ELLIS M DEVINE R KOWALSKI W DEMASSI J PRITCHARD S HROWNAK PICATINNY ARSENAL NJ 07806-5000
1	COMMANDER US ARMY ARDEC PRODUCTION BASE MODERN ACTY AMSMC PBM K PICATINNY ARSENAL NJ 07806-5000
3	COMMANDER US ARMY TACOM PM TACTICAL VEHICLES SFAE TVL SFAE TVM SFAE TVH 6501 ELEVEN MILE RD WARREN MI 48397-5000
1	COMMANDER US ARMY TACOM PM ABRAMS SFAE ASM AB 6501 ELEVEN MILE RD WARREN MI 48397-5000
1	COMMANDER US ARMY TACOM PM BFVS SFAE ASM BV 6501 ELEVEN MILE RD WARREN MI 48397-5000

NO. OF COPIES	ORGANIZATION
1	COMMANDER US ARMY TACOM PM AFAS SFAE ASM AF 6501 ELEVEN MILE RD WARREN MI 48397-5000
2	COMMANDER US ARMY TACOM PM SURV SYS SFAE ASM SS T DEAN SFAE GCSS W GSI M D COCHRAN 6501 ELEVEN MILE RD WARREN MI 48397-5000
1	COMMANDER US ARMY TACOM PM RDT&E SFAE GCSS W AB J GODELL 6501 ELEVEN MILE RD WARREN MI 48397-5000
1	COMMANDER US ARMY TACOM PM SURVIVABLE SYSTEMS SFAE GCSS W GSI H M RYZYI 6501 ELEVEN MILE RD WARREN MI 48397-5000
1	COMMANDER US ARMY TACOM PM BFV SFAE GCSS W BV S DAVIS 6501 ELEVEN MILE RD WARREN MI 48397-5000
1	COMMANDER US ARMY TACOM PM LIGHT TACTICAL VEHICLES AMSTA TR S AJ J MILLS MS 209 6501 ELEVEN MILE RD WARREN MI 48397-5000
1	COMMANDER US ARMY TACOM PM GROUND SYSTEMS INTEGRATION SFAE GCSS W GSI R LABATILLE 6501 ELEVEN MILE RD WARREN MI 48397-5000
1	COMMANDER US ARMY TACOM CHIEF ABRAMS TESTING SFAE GCSS W AB QT T KRASKIEWICZ 6501 ELEVEN MILE RD WARREN MI 48397-5000
1	COMMANDER US ARMY TACOM AMSTA SF WARREN MI 48397-5000
1	COMMANDER SMCWV QAE Q B VANINA BLDG 44 WATERVLIET ARSENAL WATERVLIET NY 12189-4050
14	COMMANDER US ARMY TACOM ASMTA TR R J CHAPIN R MCCLELLAND D THOMAS J BENNETT D HANSEN AMSTA JSK S GOODMAN J FLORENCE K IYER J THOMSON AMSTA TR D D OSTBERG L HINOJOSA B RAJU AMSTA CS SF H HUTCHINSON F SCHWARZ WARREN MI 48397-5000

NO. OF COPIES	ORGANIZATION
1	COMMANDER SMCWV SPM T MCCLOSKEY BLDG 253 WATERVLIET ARSENAL WATERVLIET NY 12189-4050
10	BENET LABS AMSTA AR CCB R FISCELLA G D ANDREA M SCAVULO G SPENCER P WHEELER K MINER J VASILAKIS G FRIAR R HASENBEIN SMCAR CCB R S SOPOK WATERVLIET NY 12189
2	TSM ABRAMS ATZK TS S JABURG W MEINSHAUSEN FT KNOX KY 40121
3	ARMOR SCHOOL ATZK TD R BAUEN J BERG A POMEY FT KNOX KY 40121
2	HQ IOC TANK AMMO TEAM AMSIO SMT R CRAWFORD W HARRIS ROCK ISLAND IL 61299-6000
1	DIRECTOR US ARMY AMCOM SFAE AV RAM TV D CALDWELL BUILDING 5300 REDSTONE ARSENAL AL 35898

NO. OF COPIES	ORGANIZATION
4	DIRECTOR US ARMY CECOM NIGHT VISION & ELECTRONIC SENSORS DIRECTORATE AMSEL RD NV CM CCD R ADAMS R MCLEAN A YINGST AMSEL RD NV VISP E JACOBS 10221 BURBECK RD FT BELVOIR VA 22060-5806
2	CDR US ARMY AMCOM AVIATION APPLIED TECH DIR J SCHUCK FT EUSTIS VA 23604-5577
1	US ARMY CRREL P DUTTA 72 LYME RD HANOVER NH 03755
1	US ARMY CERL R LAMPO 2902 NEWMARK DR CHAMPAIGN IL 61822
2	US ARMY CORP OF ENGINEERS CERD C T LIU CEW ET T TAN 20 MASS AVE NW WASHINGTON DC 20314
10	DIRECTOR US ARMY NATL GRND INTEL CTR D LEITER S EITELMAN M HOLTUS M WOLFE S MINGLEDORF H C ARDLEIGH J GASTON W GSTATTENBAUER R WARNER J CRIDER 220 SEVENTH STREET NE CHARLOTTESVILLE VA 22091

NO. OF COPIES	ORGANIZATION
6	US ARMY SBCCOM SOLDIER SYSTEMS CTR BALLISTICS TEAM J WARD MARINE CORPS TEAM J MACKIEWICZ BUS AREA ADVOCACY TEAM W HASKELL SSCNC WST W NYKVIST T MERRILL S BEAUDOIN KANSAS ST NATICK MA 01760-5019
1	US ARMY COLD REGIONS RSCH & ENGRNG LAB P DUTTA 72 LYME RD HANOVER NH 03755
1	SYSTEM MANAGER ABRAMS ATZK TS LTC J H NUNN BLDG 1002 RM 110 FT KNOX KY 40121
9	US ARMY RESEARCH OFFICE A CROWSON J CHANDRA H EVERETT J PRATER R SINGLETON G ANDERSON D STEPP D KISEROW J CHANG PO BOX 12211 RESEARCH TRIANGLE PARK NC 27709-2211
1	DIRECTORATE OF CMBT DEVELOPMENT C KJORO 320 ENGINEER LOOP STE 141 FT LEONARD WOOD MO 65473-8929

NO. OF COPIES	ORGANIZATION
1	COMMANDANT US ARMY FIELD ARTILLERY CTR ATFS CD LTC BUMGARNER FT SILL OK 73503 5600
1	CHIEF USAIC LTC T J CUMMINGS ATZB COM FT BENNING GA 31905-5800
1	NAVAL AIR SYSTEMS CMD J THOMPSON 48142 SHAW RD UNIT 5 PATUXENT RIVER MD 20670
1	NAVAL SURFACE WARFARE CTR DAHLGREN DIV CODE G06 DAHLGREN VA 22448
1	NAVAL SURFACE WARFARE CTR TECH LIBRARY CODE 323 17320 DAHLGREN RD DAHLGREN VA 22448
3	NAVAL RESEARCH LAB I WOLOCK CODE 6383 R BADALIANCE CODE 6304 L GAUSE WASHINGTON DC 20375
1	NAVAL SURFACE WARFARE CTR CRANE DIVISION M JOHNSON CODE 20H4 LOUISVILLE KY 40214-5245
2	COMMANDER NAVAL SURFACE WARFARE CTR CADEROCK DIVISION R PETERSON CODE 2020 M CRITCHFIELD CODE 1730 BETHESDA MD 20084
2	NAVAL SURFACE WARFARE CTR U SORATHIA C WILLIAMS CD 6551 9500 MACARTHUR BLVD WEST BETHESDA MD 20817

NO. OF COPIES	ORGANIZATION
1	DAVID TAYLOR RESEARCH CTR SHIP STRUCTURES & PROTECTION DEPARTMENT CODE 1702 J CORRADO BETHESDA MD 20084
2	DAVID TAYLOR RESEARCH CTR R ROCKWELL W PHYILLAIER BETHESDA MD 20054-5000
1	OFFICE OF NAVAL RESEARCH D SIEGEL CODE 351 800 N QUINCY ST ARLINGTON VA 22217-5660
8	NAVAL SURFACE WARFARE CTR J FRANCIS CODE G30 D WILSON CODE G32 R D COOPER CODE G32 J FRAYSSE CODE G33 E ROWE CODE G33 T DURAN CODE G33 L DE SIMONE CODE G33 R HUBBARD CODE G33 DAHLGREN VA 22448
1	NAVAL SEA SYSTEMS CMD D LIESE 2531 JEFFERSON DAVIS HIGHWAY ARLINGTON VA 22242-5160
1	NAVAL SURFACE WARFARE CTR M LACY CODE B02 17320 DAHLGREN RD DAHLGREN VA 22448
1	OFFICE OF NAVAL RESEARCH J KELLY 800 NORTH QUINCEY ST ARLINGTON VA 22217-5000
2	NAVAL SURFACE WARFARE CTR CARDEROCK DIVISION R CRANE CODE 2802 C WILLIAMS CODE 6553 3A LEGGETT CIR BETHESDA MD 20054-5000

NO. OF COPIES	ORGANIZATION
1	NAVSEA OJRI PEO DD21 PMS500 G CAMPONESCHI 2351 JEFFERSON DAVIS HWY ARLINGTON VA 22242-5165
1	EXPEDITIONARY WARFARE DIV N85 F SHOUP 2000 NAVY PENTAGON WASHINGTON DC 20350-2000
1	AFRL MLBC 2941 P STREET RM 136 WRIGHT PATTERSON AFB OH 45433-7750
1	AFRL MLSS R THOMSON 2179 12TH STREET RM 122 WRIGHT PATTERSON AFB OH 45433-7718
2	AFRL F ABRAMS J BROWN BLDG 653 2977 P STREET STE 6 WRIGHT PATTERSON AFB OH 45433-7739
1	AFRL MLS OL L COULTER BLDG 100 BAY D 7278 4TH STREET HILL AFB UT 84056-5205
1	OSD JOINT CCD TEST FORCE OSD JCCD R WILLIAMS 3909 HALLS FERRY RD VICKSBURG MS 29180-6199
1	DEFENSE NUCLEAR AGENCY INNOVATIVE CONCEPTS DIV R ROHR 6801 TELEGRAPH RD ALEXANDRIA VA 22310-3398

NO. OF COPIES	ORGANIZATION
1	WATERWAYS EXPERIMENT D SCOTT 3909 HALLS FERRY RD SC C VICKSBURG MS 39180
3	DARPA M VANFOSSEN S WAX L CHRISTODOULOU 3701 N FAIRFAX DR ARLINGTON VA 22203-1714
2	SERDP PROGRAM OFC PM P2 C PELLERIN B SMITH 901 N STUART ST SUITE 303 ARLINGTON VA 22203
1	FAA MIL HDBK 17 CHAIR L ILCEWICZ 1601 LIND AVE SW ANM 115N RENTON VA 98055
2	FAA TECH CTR D OPLINGER AAR 431 P SHYPRYKEVICH AAR 431 ATLANTIC CITY NJ 08405
1	OFC OF ENVIRONMENTAL MGMT US DEPT OF ENERGY P RITZCOVAN 19901 GERMANTOWN RD GERMANTOWN MD 20874-1928
1	LOS ALAMOS NATL LAB F ADDESSIO MS B216 PO BOX 1633 LOS ALAMOS NM 87545
1	OAK RIDGE NATL LAB R M DAVIS PO BOX 2008 OAK RIDGE TN 37831-6195
5	DIRECTOR LAWRENCE LIVERMORE NATL LAB R CHRISTENSEN S DETERESA F MAGNESS M FINGER MS 313 M MURPHY L 282 PO BOX 808 LIVERMORE CA 94550
7	NIST R PARNAS J DUNKERS M VANLANDINGHAM MS 8621 J CHIN MS 8621 D HUNSTON MS 8543 J MARTIN MS 8621 D DUTHINH MS 8611 100 BUREAU DR GAITHERSBURG MD 20899
1	OAK RIDGE NATL LAB C EBERLE MS 8048 PO BOX 2009 OAK RIDGE TN 37831
1	OAK RIDGE NATL LAB C D WARREN MS 8039 PO BOX 2009 OAK RIDGE TN 37922
4	DIRECTOR SANDIA NATL LABS APPLIED MECHANICS DEPT DIVISION 8241 W KAWAHARA K PERANO D DAWSON P NIELAN PO BOX 969 LIVERMORE CA 94550-0096
1	LAWRENCE LIVERMORE NATIONAL LAB M MURPHY PO BOX 808 L 282 LIVERMORE CA 94550

NO. OF COPIES	ORGANIZATION
3	NASA LANGLEY RESEARCH CTR MS 266 AMSRL VS W ELBER F BARTLETT JR G FARLEY HAMPTON VA 23681-0001
1	NASA LANGLEY RESEARCH CTR T GATES MS 188E HAMPTON VA 23661-3400
1	USDOT FEDERAL RAILROAD RDV 31 M FATEH WASHINGTON DC 20590
1	DOT FHWA J SCALZI 400 SEVENTH ST SW 3203 HNG 32 WASHINGTON DC 20590
1	FHWA E MUNLEY 6300 GEORGETOWN PIKE MCLEAN VA 22101
1	CENTRAL INTELLIGENCE AGENCY OTI WDAG GT W L WALTMAN PO BOX 1925 WASHINGTON DC 20505
1	MARINE CORPS INTEL ACTY D KOSITZKE 3300 RUSSELL RD SUITE 250 QUANTICO VA 22134-5011
1	NATL GRND INTELLIGENCE CTR DIRECTOR IANG TMT 220 SEVENTH ST NE CHARLOTTESVILLE VA 22902-5396
1	DIRECTOR DEFENSE INTELLIGENCE AGENCY TA 5 K CRELLING WASHINGTON DC 20310

NO. OF COPIES	ORGANIZATION
1	GRAPHITE MASTERS INC J WILLIS 3815 MEDFORD ST LOS ANGELES CA 90063-1900
1	ADVANCED GLASS FIBER YARNS T COLLINS 281 SPRING RUN LN STE A DOWNINGTON PA 19335
1	COMPOSITE MATERIALS INC D SHORTT 19105 63 AVE NE PO BOX 25 ARLINGTON WA 98223
1	COMPOSITE MATERIALS INC R HOLLAND 11 JEWEL COURT ORINDA CA 94563
1	COMPOSITE MATERIALS INC C RILEY 14530 S ANSON AVE SANTA FE SPRINGS CA 90670
2	COMPOSIX D BLAKE L DIXON 120 O NEILL DR HEBRUN OHIO 43025
4	CYTEC FIBERITE R DUNNE D KOHLI M GILLIO R MAYHEW 1300 REVOLUTION ST HAVRE DE GRACE MD 21078
2	SIMULA J COLTMAN R HUYETT 10016 S 51ST ST PHOENIX AZ 85044
1	SIOUX MFG B KRIEL PO BOX 400 FT TOTTEN ND 58335

NO. OF COPIES	ORGANIZATION
2	PROTECTION MATERIALS INC M MILLER F CRILLEY 14000 NW 58 CT MIAMI LAKES FL 33014
3	FOSTER MILLER J J GASSNER M ROYLANCE W ZUKAS 195 BEAR HILL RD WALTHAM MA 02354-1196
1	ROM DEVELOPMENT CORP R O MEARA 136 SWINEBURNE ROW BRICK MARKET PLACE NEWPORT RI 02840
2	TEXTRON SYSTEMS T FOLTZ M TREASURE 201 LOWELL ST WILMINGTON MA 08870-2941
1	JPS GLASS L CARTER PO BOX 260 SLATER RD SLATER SC 29683
1	O GARA HESS & EISENHARDT M GILLESPIE 9113 LESAINT DR FAIRFIELD OH 45014
2	MILLIKEN RESEARCH CORP H KUHN M MACLEOD PO BOX 1926 SPARTANBURG SC 29303
1	CONNEAUGHT INDUSTRIES INC J SANTOS PO BOX 1425 COVENTRY RI 02816

NO. OF COPIES	ORGANIZATION
1	BATTELLE C R HARGREAVES 505 KING AVE COLUMBUS OH 43201-2681
2	BATTELLE NATICK OPERATIONS J CONNORS B HALPIN 209 W CENTRAL ST STE 302 NATICK MA 01760
1	BATTELLE NW DOE PNNL T HALL MS K231 BATTELLE BLVD RICHLAND WA 99352
3	PACIFIC NORTHWEST LAB M SMITH G VAN ARSDALE R SHIPPELL PO BOX 999 RICHLAND WA 99352
1	ARMTEC DEFENSE PRODUCTS S DYER 85 901 AVE 53 PO BOX 848 COACHELLA CA 92236
2	ADVANCED COMPOSITE MATLS CORP P HOOD J RHODES 1525 S BUNCOMBE RD GREER SC 29651-9208
2	GLCC INC J RAY M BRADLEY 103 TRADE ZONE DR STE 26C WEST COLUMBIA SC 29170
2	AMOCO PERFORMANCE PRODUCTS M MICHNO JR J BANISAUKAS 4500 MCGINNIS FERRY RD ALPHARETTA GA 30202-3944

NO. OF COPIES	ORGANIZATION
1	SAIC M PALMER 2109 AIR PARK RD S E ALBUQUERQUE NM 87106
1	SAIC G CHRYSSOMALLIS 3800 W 80TH ST STE 1090 BLOOMINGTON MN 55431
1	AAI CORPORATION T G STASTNY PO BOX 126 HUNT VALLEY MD 21030-0126
1	JOHN HEBERT PO BOX 1072 HUNT VALLEY MD 21030-0126
12	ALLIANT TECHSYSTEMS INC C CANDLAND C AAKHUS R BECKER B SEE N VLAHAKUS R DOHRN S HAGLUND D FISHER W WORRELL R COPENHAFER M HISSONG D KAMDAR 600 2ND ST NE HOPKINS MN 55343-8367
3	ALLIANT TECHSYSTEMS INC J CONDON E LYNAM J GERHARD WV01 16 STATE RT 956 PO BOX 210 ROCKET CENTER WV 26726-0210
1	APPLIED COMPOSITES W GRISCH 333 NORTH SIXTH ST ST CHARLES IL 60174

NO. OF COPIES	ORGANIZATION
1	PROJECTILE TECHNOLOGY INC 515 GILES ST HAVRE DE GRACE MD 21078
1	CUSTOM ANALYTICAL ENG SYS INC A ALEXANDER 13000 TENSOR LN NE FLINTSTONE MD 21530
2	LORAL VOUGHT SYSTEMS G JACKSON K COOK 1701 W MARSHALL DR GRAND PRAIRIE TX 75051
5	AEROJET GEN CORP D PILLASCH T COULTER C FLYNN D RUBAREZUL M GREINER 1100 WEST HOLLYVALE ST AZUSA CA 91702-0296
3	HEXCEL INC R BOE F POLICELLI J POESCH PO BOX 98 MAGNA UT 84044
3	HERCULES INC G KUEBELER J VERMEYCHUK B MANDERVILLE JR HERCULES PLAZA WILMINGTON DE 19894
1	BRIGS COMPANY J BACKOFEN 2668 PETERBOROUGH ST HERNDON VA 22071-2443
1	ZERNOW TECHNICAL SERVICES L ZERNOW 425 W BONITA AVE STE 208 SAN DIMAS CA 91773

NO. OF COPIES	ORGANIZATION
2	OLIN CORPORATION FLINCHBAUGH DIV E STEINER B STEWART PO BOX 127 RED LION PA 17356
1	OLIN CORPORATION L WHITMORE 10101 9TH ST NORTH ST PETERSBURG FL 33702
1	DOW UT S TIDRICK 15 STERLING DR WALLINGFORD CT 06492
5	SIKORSKY AIRCRAFT G JACARUSO T CARSTENSAN B KAY S GARBO M S S330A J ADELMANN 6900 MAIN ST PO BOX 9729 STRATFORD CT 06497-9729
1	PRATT & WHITNEY D HAMBRICK 400 MAIN ST MS 114 37 EAST HARTFORD CT 06108
1	AEROSPACE CORP G HAWKINS M4 945 2350 E EL SEGUNDO BLVD EL SEGUNDO CA 90245
2	CYTEC FIBERITE M LIN W WEB 1440 N KRAEMER BLVD ANAHEIM CA 92806
1	HEXCEL T BITZER 11711 DUBLIN BLVD DUBLIN CA 94568

NO. OF COPIES	ORGANIZATION
1	BOEING R BOHLMANN PO BOX 516 MC 5021322 ST LOUIS MO 63166-0516
2	BOEING DEFENSE & SPACE GRP W HAMMOND J RUSSELL S 4X55 PO BOX 3707 SEATTLE WA 98124-2207
2	BOEING ROTORCRAFT P MINGURT P HANDEL 800 B PUTNAM BLVD WALLINGFORD PA 19086
1	BOEING DOUGLAS PRODUCTS DIV L J HART SMITH 3855 LAKEWOOD BLVD D800 0019 LONG BEACH CA 90846-0001
1	LOCKHEED MARTIN S REEVE 8650 COBB DR D 73 62 MZ 0648 MARIETTA GA 30063-0648
1	LOCKHEED MARTIN SKUNK WORKS D FORTNEY 1011 LOCKHEED WAY PALMDALE CA 93599-2502
1	LOCKHEED MARTIN R FIELDS 1195 IRWIN CT WINTER SPRINGS FL 32708
1	MATERIALS SCIENCES CORP B W ROSEN 500 OFFICE CENTER DR STE 250 FORT WASHINGTON PA 19034

NO. OF COPIES	ORGANIZATION
1	NORTHROP GRUMMAN CORP ELECTRONIC SENSORS & SYSTEMS DIV E SCHOCH MAILSTOP V 16 1745A WEST NURSERY RD LINTHICUM MD 21090
2	NORTHROP GRUMMAN ENVIRONMENTAL PROGRAMS R OSTERMAN A YEN 8900 E WASHINGTON BLVD PICO RIVERA CA 90660
1	UNITED DEFENSE LP D MARTIN PO BOX 359 SANTA CLARA CA 95052
1	UNITED DEFENSE LP G THOMAS PO BOX 58123 SANTA CLARA CA 95052
2	UNITED DEFENSE LP R BARRETT V HORVATICH MAIL DROP M53 328 W BROKAW RD SANTA CLARA CA 95052-0359
3	UNITED DEFENSE LP GROUND SYSTEMS DIVISION M PEDRAZZI MAIL DROP N09 A LEE MAIL DROP N11 M MACLEAN MAIL DROP N06 1205 COLEMAN AVE SANTA CLARA CA 95052
4	UNITED DEFENSE LP 4800 EAST RIVER RD R BRYNSVOLD P JANKE MS170 T GIOVANETTI MS236 B VAN WYK MS389 MINNEAPOLIS MN 55421-1498
2	GENERAL DYNAMICS LAND SYSTEMS D REES M PASIK PO BOX 2074 WARREN MI 48090-2074
1	GENERAL DYNAMICS LAND SYSTEMS D BARTLE PO BOX 1901 WARREN MI 48090
1	GENERAL DYNAMICS LAND SYSTEMS MUSKEGON OPERATIONS W SOMMERS JR 76 GETTY ST MUSKEGON MI 49442
1	GENERAL DYNAMICS AMPHIBIOUS SYS SURVIVABILITY LEAD G WALKER 991 ANNAPOLIS WAY WOODBRIDGE VA 22191
5	INST FOR ADVANCED TECH T KIEHNE H FAIR P SULLIVAN W REINECKE I MCNAB 4030 2 W BRAKER LN AUSTIN TX 78759
2	CIVIL ENGR RSCH FOUNDATION H BERNSTEIN PRESIDENT R BELLE 1015 15TH ST NW STE 600 WASHINGTON DC 20005
1	ARROW TECH ASSO 1233 SHELBURNE RD STE D 8 SOUTH BURLINGTON VT 05403-7700

NO. OF COPIES	ORGANIZATION
1	CONSULTANT R EICHELBERGER 409 W CATHERINE ST BEL AIR MD 21014-3613
1	UCLA MANE DEPT ENGR IV H THOMAS HAHN LOS ANGELES CA 90024-1597
2	UNIV OF DAYTON RESEARCH INST RAN Y KIM AJIT K ROY 300 COLLEGE PARK AVE DAYTON OH 45469-0168
1	MIT P LAGACE 77 MASS AVE CAMBRIDGE MA 01887
1	IIT RESEARCH CTR D ROSE 201 MILL ST ROME NY 13440-6916
1	GEORGIA TECH RESEARCH INST GEORGIA INST OF TECHNOLOGY P FRIEDERICH ATLANTA GA 30392
1	MICHIGAN ST UNIV R AVERILL 3515 EB MSM DEPT EAST LANSING MI 48824-1226
1	UNIV OF KENTUCKY L PENN 763 ANDERSON HALL LEXINGTON KY 40506-0046
1	UNIV OF WYOMING D ADAMS PO BOX 3295 LARAMIE WY 82071

NO. OF COPIES	ORGANIZATION
1	UNIV OF UTAH DEPT OF MECH & INDUSTRIAL ENGR S SWANSON SALT LAKE CITY UT 84112
2	PENNSYLVANIA STATE UNIV R MCNITT C BAKIS 227 HAMMOND BLDG UNIVERSITY PARK PA 16802
1	PENNSYLVANIA STATE UNIV RENATA S ENGEL 245 HAMMOND BLDG UNIVERSITY PARK PA 16801
1	PURDUE UNIV SCHOOL OF AERO & ASTRO C T SUN W LAFAYETTE IN 47907-1282
1	STANFORD UNIV DEPARTMENT OF AERONAUTICS AND AEROBALLISTICS DURANT BUILDING S TSAI STANFORD CA 94305
1	UNIV OF DAYTON J M WHITNEY COLLEGE PARK AVE DAYTON OH 45469-0240
7	UNIV OF DELAWARE CTR FOR COMPOSITE MATRLS J GILLESPIE M SANTARE G PALMESE S YARLAGADDA S ADVANI D HEIDER D KUKICH 201 SPENCER LABORATORY NEWARK DE 19716

NO. OF COPIES	ORGANIZATION
1	UNIV OF ILLINOIS AT URBANA CHAMPAIGN NATL CTR FOR COMPOSITE MATERIALS RESEARCH 216 TALBOT LABORATORY J ECONOMY 104 S WRIGHT ST URBANA IL 61801
3	THE UNIV OF TEXAS AT AUSTIN CTR FOR ELECTROMECHANICS J PRICE A WALLS J KITZMILLER 10100 BURNET RD AUSTIN TX 78758-4497
3	VA POLYTECHNICAL INST STATE UNIV DEPT OF ESM M W HYER K REIFSNIDER R JONES BLACKSBURG VA 24061-0219
1	NORTH CAROLINA STATE UNIV CIVIL ENGINEERING DEPT W RASDORF PO BOX 7908 RALEIGH NC 27696-7908
1	UNIV OF MARYLAND DEPT OF AEROSPACE ENGINEERING ANTHONY J VIZZINI COLLEGE PARK MD 20742
1	DREXEL UNIV ALBERT S D WANG 32ND AND CHESTNUT STREETS PHILADELPHIA PA 19104
1	SOUTHWEST RSCH INST ENGR & MATL SCIENCES DIV J RIEGEL 6220 CULEBRA RD PO DRAWER 28510 SAN ANTONIO TX 78228-0510

NO. OF COPIES	ORGANIZATION
	ABERDEEN PROVING GROUND
1	COMMANDER US ARMY MATERIEL SYS ANALYSIS P DIETZ 392 HOPKINS RD AMXSY TD APG MD 21005-5071
1	DIRECTOR US ARMY RESEARCH LAB AMSRL OP AP L APG MD 21005 5066
115	DIR USARL AMSRL CI AMSRL CI H W STUREK AMSRL CI S A MARK AMSRL CS IO FI M ADAMSON AMSRL SL B J SMITH AMSRL SL BA AMSRL SL BL D BELY R HENRY AMSRL SL BG A YOUNG AMSRL SL I AMSRL WM B A HORST E SCHMIDT AMSRL WM BA W D AMICO F BRANDON AMSRL WM BC P PLOSTINS D LYON J NEWILL S WILKERSON A ZIELINSKI AMSRL WM BD B FORCH R FIFER R PESCE RODRIGUEZ B RICE

NO. OF COPIES	ORGANIZATION
	ABERDEEN PROVING GROUND (CONT)
	AMSRL WM BE
	G WREN
	C LEVERITT
	D KOOKER
	AMSRL WM BR
	C SHOEMAKER
	J BORNSTEIN
	AMSRL WM M
	D VIECHNICKI
	G HAGNAUER
	J MCCAULEY
	B TANNER
	AMSRL WM MA
	R SHUFORD
	P TOUCHET
	N BECK TAN
	D FLANAGAN
	L GHIORSE
	D HARRIS
	S MCKNIGHT
	P MOY
	S NGYUEN
	P PATTERSON
	G RODRIGUEZ
	A TEETS
	R YIN
	AMSRL WM MB
	B FINK
	J BENDER
	T BLANAS
	T BOGETTI
	R BOSSOLI
	L BURTON
	K BOYD
	S CORNELISON
	P DEHMER
	R DOOLEY
	W DRYSDALE
	G GAZONAS
	S GHIORSE
	D GRANVILLE
	D HOPKINS
	C HOPPEL
	D HENRY
	R KASTE
	M KLUSEWITZ
	M LEADORE
	R LIEB

NO. OF COPIES	ORGANIZATION
	ABERDEEN PROVING GROUND (CONT)
	AMSRL WM MB
	E RIGAS
	J SANDS
	D SPAGNUOLO
	W SPURGEON
	J TZENG
	E WETZEL
	A ABRAHAMIAN
	M BERMAN
	A FRYDMAN
	T LI
	W MCINTOSH
	E SZYMANSKI
	AMRSL WM MC
	J BEATTY
	J SWAB
	E CHIN
	J MONTGOMERY
	A WERESCZCAK
	J LASALVIA
	J WELLS
	AMSRL WM MD
	W ROY
	S WALSH
	AMSRL WM T
	B BURNS
	AMSRL WM TA
	W GILLICH
	T HAVEL
	J RUNYEON
	M BURKINS
	E HORWATH
	B GOOCH
	W BRUCHEY
	AMSRL WM TC
	R COATES
	AMSRL WM TD
	A DAS GUPTA
	T HADUCH
	T MOYNIHAN
	F GREGORY
	A RAJENDRAN
	M RAFTENBERG
	M BOTELER
	T WEERASOORIYA
	D DANDEKAR
	A DIETRICH

NO. OF
COPIES ORGANIZATION

ABERDEEN PROVING GROUND (CONT)

AMSRL WM TE
A NIILER
J POWELL
AMSRL SS SD
H WALLACE
AMSRL SS SE R
R CHASE
AMSRL SS SE DS
R REYZER
R ATKINSON
AMSRL SE L
R WEINRAUB
J DESMOND
D WOODBURY

NO. OF COPIES	ORGANIZATION
1	R MARTIN MERL LTD TAMWORTH RD HERTFORD SG13 7DG UNITED KINGDOM
1	PW LAY SMC SCOTLAND DERA ROSYTH ROSYTH ROYAL DOCKYARD DUNFERMLINE FIFE KY 11 2XR UNITED KINGDOM
1	T GOTTESMAN CIVIL AVIATION ADMINISTRATION PO BOX 8 BEN GURION INTERNL AIRPORT LOD 70150 ISRAEL
1	S ANDRE AEROSPATIALE A BTE CC RTE MD132 316 ROUTE DE BAYONNE TOULOUSE 31060 FRANCE
1	J BAUER DAIMLER BENZ AEROSPACE D 81663 MUNCHEN MUNICH GERMANY
3	DRA FORT HALSTEAD PETER N JONES DAVID SCOTT MIKE HINTON SEVEN OAKS KENT TN 147BP UNITED KINGDOM
1	FRANCOIS LESAGE DEFENSE RESEARCH ESTAB VALCARTIER PO BOX 8800 COURCELETTE QUEBEC COA IRO CANADA

NO. OF COPIES	ORGANIZATION
2	ROYAL MILITARY COLLEGE OF SCIENCE SHRIVENHAM D BULMAN B LAWTON SWINDON WILTS SN6 8LA UNITED KINGDOM
1	SWISS FEDERAL ARMAMENTS WKS WALTER LANZ ALLMENDSTRASSE 86 3602 THUN SWITZERLAND
1	PROFESSOR SOL BODNER ISRAEL INST OF TECHNOLOGY FACULTY OF MECHANICAL ENGR HAIFA 3200 ISRAEL
1	DSTO MATERIALS RSRCH LAB DR NORBERT BURMAN NAVAL PLATFORM VULNERABILITY SHIP STRUCTURES & MATERIALS DIV PO BOX 50 ASCOT VALE VICTORIA AUSTRALIA 3032
1	PROFESSOR EDWARD CELENS ECOLE ROYAL MILITAIRE AVE DE LA RENAISSANCE 30 1040 BRUXELLE BELGIQUE
1	DEF RES ESTABLISHMENT VALCARTIER ALAIN DUPUIS 2459 BOULEVARD PIE XI NORTH VALCARTIER QUEBEC CANADA PO BOX 8800 COURCELETTE GOA IRO QUEBEC CANADA

NO. OF COPIES	ORGANIZATION
1	INSTITUT FRANCO ALLEMAND DE RECHERCHES DE SANIT LOUIS DE MARC GIRAUD RUE DU GENERAL CASSAGNOU BOITE POSTALE 34 F 68301 SAINT LOUIS CEDEX FRANCE
1	J MANSON ECOLE POLYTECH DMX LTC CH 1015 LAUSANNE SWITZERLAND
1	TNO PRINS MAURITS LAB ROB IJSSELSTEIN LANGE KLEIWEG 137 PO BOX 45 2280 AA RIJSWIJK THE NETHERLANDS
2	FOA NAT L DEFENSE RESEARCH ESTAB BO JANZON R HOLMLIN DIR DEPT OF WEAPONS & PROTECTION S 172 90 STOCKHOLM SWEDEN
2	DEFENSE TECH & PROC AGENCY GRND I CREWTHER GENERAL HERZOG HAUS 3602 THUN SWITZERLAND
1	MINISTRY OF DEFENCE RAFAEL MEIR MAYSELESS ARMAMENT DEVELOPMENT AUTH PO BOX 2250 HAIFA 31021 ISRAEL
1	AKE PERSSON DYNAMEC RESEARCH AB PARADISGRND 7 S 151 36 SODERTALJE SWEDEN

NO. OF COPIES	ORGANIZATION
1	ERNST MACH INSTITUT EMI DIRECTOR HAUPTSTRASSE 18 79576 WEIL AM RHEIN GERMANY
1	ERNST MACH INSTITUT EMI ALOIS STILP ECKERSTRASSE 4 7800 FREIBURG GERMANY
1	IR HANS PASMAN TNO DEFENSE RESEARCH POSTBUS 6006 2600 JA DELFT THE NETHERLANDS
1	BITAN HIRSCH TACHKEMONY ST 6 NETAMUA 42611 ISRAEL
1	MANFRED HELD DEUTSCHE AEROSPACE AG DYNAMICS SYSTEMS PO BOX 1340 D 86523 SCHROBENHAUSEN GERMANY

REPORT DOCUMENTATION PAGE

Form Approved
OMB No. 0704-0188

1. AGENCY USE ONLY *(Leave blank)*	2. REPORT DATE	3. REPORT TYPE AND DATES COVERED
	September 2000	Final, Jan 95 - Dec 98

4. TITLE AND SUBTITLE
Induction Heating of Carbon-Fiber Composites: Thermal Generation Model

5. FUNDING NUMBERS
AH42

6. AUTHOR(S)
Bruce K. Fink, Roy L. McCullough,* and John W. Gillespie, Jr.*

7. PERFORMING ORGANIZATION NAME(S) AND ADDRESS(ES)
U.S. Amy Research Laboratory
AMSRL-WM-MB
Aberdeen Proving Ground, MD 21005-5069

8. PERFORMING ORGANIZATION REPORT NUMBER
ARL-TR-2261

9. SPONSORING/MONITORING AGENCY NAMES(S) AND ADDRESS(ES)

10.SPONSORING/MONITORING AGENCY REPORT NUMBER

11. SUPPLEMENTARY NOTES
*University of Delaware, Newark, DE 19716

12a. DISTRIBUTION/AVAILABILITY STATEMENT
Approved for public release; distribution is unlimited.

12b. DISTRIBUTION CODE

13. ABSTRACT *(Maximum 200 words)*

A theory of local and global mechanisms of heat generation and distribution in carbon-fiber-based composites subjected to an alternating magnetic field has been proposed. A model that predicts the strength and distribution of thermal generation through the thickness of carbon-fiber-based laminated composites has been developed. Earlier work has established the distribution of point voltages in the plane of the laminate that exist in the form of potential differences between fibers in adjacent plies in a cross-ply or angle-ply laminate system. In this work, a capacitive-layer microstructure that models the actual fiber-reinforced-polymer microstructure from a square-packing assumption to a series of conductive parallel plates is formulated. An effective parameter of heating, gamma, that establishes the distribution of heating through the thickness is defined. Extreme gradients in this thermal source can exist with peaks occurring at the interfaces of ply-ply orientation changes. An optimization study establishes the effect of various microstructural and macrostructural parameters on the heating parameter, gamma. Several parametric studies are performed on the computer algorithm, which calculates gamma to further analyze these effects.

14. SUBJECT TERMS	15. NUMBER OF PAGES
carbon fiber, induction heating, composites	51
	16. PRICE CODE

17. SECURITY CLASSIFICATION OF REPORT	18. SECURITY CLASSIFICATION OF THIS PAGE	19. SECURITY CLASSIFICATION OF ABSTRACT	20. LIMITATION OF ABSTRACT
UNCLASSIFIED	UNCLASSIFIED	UNCLASSIFIED	UL